Long-term trends of inorganic chlorine from ground-based infrared solar spectra: Past increases and evidence for stabilization

C. P. Rinsland,[1] E. Mahieu,[2] R. Zander,[2] N. B. Jones,[3] M. P. Chipperfield,[4] A. Goldman,[5] J. Anderson,[6] J. M. Russell III,[6] P. Demoulin,[2] J. Notholt,[7] G. C. Toon,[8] J.-F. Blavier,[8] B. Sen,[8] R. Sussmann,[9] S. W. Wood,[10] A. Meier,[3] D. W. T. Griffith,[3] L. S. Chiou,[11] F. J. Murcray,[5] T. M. Stephen,[5] F. Hase,[12] S. Mikuteit,[12] A. Schulz,[13] and T. Blumenstock[12]

[1] Long-term time series of hydrogen chloride (HCl) and chlorine nitrate ($ClONO_2$) total column abundances has been retrieved from high spectral resolution ground-based solar absorption spectra recorded with infrared Fourier transform spectrometers at nine NDSC (Network for the Detection of Stratospheric Change) sites in both Northern and Southern Hemispheres. The data sets span up to 24 years and most extend until the end of 2001. The time series of Cl_y (defined here as the sum of the HCl and $ClONO_2$ columns) from the three locations with the longest time-span records show rapid increases until the early 1990s superimposed on marked day-to-day, seasonal and inter-annual variability. Subsequently, the buildup in Cl_y slows and reaches a broad plateau after 1996, also characterized by variability. A similar time evolution is also found in the total chlorine concentration at 55 km altitude derived from Halogen Occultation Experiment (HALOE) global observations since 1991. The stabilization of inorganic chlorine observed in both the total columns and at 55 km altitude indicates that the near-global 1993 organic chlorine (CCl_y) peak at the Earth's surface has now propagated over a broad altitude range in the upper atmosphere, though the time lag is difficult to quantify precisely from the current data sets, due to variability. We compare the three longest measured time series with two-dimensional model calculations extending from 1977 to 2010, based on a halocarbon scenario that assumes past measured trends and a realistic extrapolation into the future. The model predicts broad Cl_y maxima consistent with the long-term observations, followed by a slow Cl_y decline reaching 12–14% relative to the peak by 2010. The data reported here confirm the effectiveness of the Montreal Protocol and its Amendments and Adjustments in progressively phasing out the major man-related perturbations of the stratospheric ozone layer, in particular, the anthropogenic chlorine-bearing source gases. *INDEX TERMS:* 0325 Atmospheric Composition and Structure: Evolution of the atmosphere; 0322 Atmospheric Composition and Structure: Constituent sources and sinks; 0340 Atmospheric Composition and Structure: Middle atmosphere—composition and chemistry; 0345 Atmospheric Composition and Structure: Pollution—urban and regional (0305)

[1]NASA Langley Research Center, Hampton, Virginia, USA.

[2]Institute of Astrophysics and Geophysics, University of Liège, Liège, Belgium.

[3]Department of Chemistry, University of Wollongong, Wollongong, New South Wales, Australia.

[4]School of the Environment, University of Leeds, Leeds, UK.

[5]Department of Physics, University of Denver, Denver, Colorado, USA.

[6]Department of Physics, Center for Atmospheric Sciences, Hampton University, Hampton, Virginia, USA.

[7]Institute of Environmental Physics, University of Bremen, Bremen, Germany.

[8]Jet Propulsion Laboratory, Pasadena, California, USA.

[9]Institute of Meteorology and Climate Research IMK-IFU, Forschungszentrum Karlsruhe, Garmisch-Partenkirchen, Germany.

[10]National Institute for Water and Atmospheric Research, Lauder, New Zealand.

[11]Science Applications International Corporation, Hampton, Virginia, USA.

[12]Institute of Meteorology and Climate Research IMK-ASF, Forschungszentrum Karlsruhe, Karlsruhe, Germany.

[13]Alfred Wegener Institute for Polar and Marine Research, Potsdam, Germany.

1. Introduction

[2] Since the mid-1970s, the inorganic chlorine (Cl_y) loading in the stratosphere, primarily made up of hydrogen chloride (HCl) and chlorine nitrate ($ClONO_2$), has been recognized as an important factor triggering changes in the Earth's middle atmosphere, in particular, the erosion of the ozone layer. Although numerous natural sources of gaseous HCl exist at the ground [e.g., *Ryan and Mukherjee*, 1975], the current stratospheric HCl burden results primarily from the photodissociation by UV radiation of industrial emissions of chlorofluorocarbons (CFCs), hydrochlorofluorocarbons (HCFCs), carbon tetrachloride (CCl_4), and methyl chloroform (CH_3CCl_3) [e.g., *Molina and Rowland*, 1974; *Crutzen et al.*, 1978]. Secondary sources of stratospheric HCl are the decomposition of CH_3Cl (methyl chloride) released from marine algae [e.g., *Cicerone*, 1981] and the burning of vegetation [e.g., *Penkett et al.*, 1980]. Direct injection of HCl from powerful volcanic eruptions is an infrequent source of stratospheric chlorine [*Mankin and Coffey*, 1984; *Mankin et al.*, 1992; *Coffey*, 1996].

[3] Recognizing the anthropogenic dominance of these source gas emissions into the atmosphere [*World Meteorological Organization* (*WMO*), 1986], the Montreal Protocol and its strengthening Amendments and Adjustments (http://www.unep.org/ozone/montreal.shtml) have been implemented to progressively limit and then phase-out the production (and consequently the emissions) of all halogenated source gases with large ozone depleting potentials (ODPs). Within this context, stratospheric HCl and $ClONO_2$ play crucial roles in the O_3 catalytic cycle where they act as temporary reservoirs of chlorine atoms. In general, the partitioning of total inorganic chlorine (Cl_y = HCl + $ClONO_2$ + ClO + OClO + HOCl + Cl + ...) favors the reservoir species over the shorter-lived, highly reactive species (Cl_x = ClO + Cl + OClO) that efficiently destroy ozone [*World Meteorological Organization* (*WMO*), 1999]. The turnover in the stratospheric inorganic chlorine burden is a milestone for quantifying the effectiveness of these international regulations. The long-term ground-based monitoring of HCl and $ClONO_2$ burdens is among the high priority tasks of the Network for the Detection of Stratospheric Change (NDSC) [*Kurylo*, 1991; *Kurylo and Zander*, 2000; URL: http://www.ndsc.ws], along with the comparison of such measurements with correlative space-based observations for validation purposes [*Zander et al.*, 1993b, 1999; *Russell et al.*, 1996].

[4] High spectral resolution infrared solar absorption spectrometry has long been recognized as a key technique for remotely measuring atmospheric HCl from the ground, airplanes, and balloons [*Farmer et al.*, 1976; *Ackerman et al.*, 1976; *Mankin and Coffey*, 1983] and subsequently from space [e.g., *Raper et al.*, 1987; *Zander et al.*, 1992, 1996; *Gunson et al.*, 1994; *Russell et al.*, 1996] by observing the strong HCl (1−0) band transitions located near 3 μm. Past investigations of HCl trends from long-term ground-based monitoring include the studies by *Zander et al.* [1987], *Rinsland et al.* [1991], *Wallace and Livingston* [1991], and *Wallace et al.* [1997]. All of these papers reported HCl total column increases obtained mostly prior to the impact of the regulations noted above. Hence they do not reflect the related changes in chlorinated stratospheric loading that have occurred recently.

[5] After HCl, chlorine nitrate is the most abundant temporary inorganic chlorine reservoir in the stratosphere, also inhibiting ozone destruction by the Cl_x catalytic cycle. Its presence in the atmosphere was first unambiguously confirmed by the identification of its three strongest IR absorption bands in Atmospheric Trace Molecule Spectroscopy (ATMOS) solar occultation spectra recorded during the 1985 Spacelab 3 mission [*Zander et al.*, 1986]. Since that time, methods have been developed for measuring $ClONO_2$ total columns from ground-based infrared solar spectra using the ν_4 band Q branch at 780.22 cm^{-1} [*Reisinger et al.*, 1995], the feature best suited for such analysis in the midinfrared [*Farmer et al.*, 1987; *Zander and Demoulin*, 1988; *Rinsland et al.*, 1996].

[6] Recently, *Anderson et al.* [2000] reported near-global Cl_y derived from Halogen Occultation Experiment (HALOE) [*Russell et al.*, 1993] observations of HCl mixing ratios at 55 km altitude (∼0.5 hPa). The time series show that Cl_y near the stratopause increased rapidly during 1992−1996 followed by a sharp decline at the start of 1997. The turnover was interpreted as a response to the decrease in the near-surface background global organic chlorine burden, CCl_y, which occurred between 1992 and 1994 [*Montzka et al.*, 1996, 1999; *Prinn et al.*, 2000, section 4]. However, *Waugh et al.* [2001] pointed out that the observed near-global evolution in the HALOE Cl_y concentration at 55 km should be consistent with a troposphere-to-upper stratospheric time lag of about 6 years, thus peaking in late 1999 rather than in early 1997 as observed. *Waugh et al.* [2001] further commented that the HALOE 1997 Cl_y turnover was much sharper than expected from model calculations.

[7] The goal of this work is to report and interpret time series of HCl and $ClONO_2$ total vertical column abundances derived from ground-based infrared solar absorption spectra observed with Fourier Transform Infrared (FTIR) instruments at nine NDSC sites encompassing latitudes from 78.9°N to 45.0°S. The time series span up to 24 years with all databases extending to the end of 2001. They are analyzed to quantify the long-term trend in total inorganic chlorine loading.

[8] The NDSC Cl_y total column and HALOE 55 km time series will be compared with global average background CCl_y near the surface [*Prinn et al.*, 2000] to test the agreement between both sets of measurements when assuming realistic lag times for transport of surface air to stratospheric altitudes at different latitudes. The Cl_y total columns from the three longest NDSC time series will be further compared with two-dimensional (2-D) chemical-dynamical-radiative model calculations spanning 1977−2010. The model used a realistic halocarbon scenario based on past observations and a best estimate of future emissions. The model was initialized with sulfate aerosol loadings based primarily on Stratospheric Aerosol Measurements (SAM) II, Stratospheric Aerosol and Gas

Experiment (SAGE) I, and SAGE II observations. After 1995, the model assumes the 1995 aerosol loading, though in reality it has continued to decrease.

2. Methodology

[9] The present work reports long-term HCl and $ClONO_2$ vertical column abundance measurements retrieved from high spectral resolution FTIR solar observations with similar analysis approaches and spectroscopic parameters. The aim is to ensure that the time changes observed at the participating sites can be intercompared and lead to consistent trend-related conclusions. All of the reported HCl measurements were obtained in the 3-μm domain where the strong HCl (1-0) band lines are located. Retrievals of $ClONO_2$ columns were obtained from fits to the ν_4 band Q branch at 780.22 cm^{-1}.

[10] Most of the retrievals were performed with the "SFIT1" or "SFIT2" algorithms, which share a common forward model and atmospheric ray tracing code. These algorithms use density-weighted pressures and temperatures for 29 or more atmospheric layers extending from the stations' altitudes to 100 km, based on the "FSCATM" air mass computer program [*Gallery et al.*, 1983; *Meier et al.*, 2003]. The SFIT1 code [*Rinsland et al.*, 1982] retrieves total columns of up to five species from nonlinear least squares fits to individual spectra in a single microwindow by scaling a priori profiles by single multiplicative factors over all layers. The SFIT2 algorithm [*Pougatchev et al.*, 1995; *Connor et al.*, 1996; *Rinsland et al.*, 1998, 2000a, 2000b] assumes the formalism of *Rodgers* [1990], modified based on its semiempirical implementation [*Parrish et al.*, 1992; *Connor et al.*, 1995]. The vertical profiles of one or two target species can be retrieved simultaneously from fits to one or more microwindows. The total column of each interfering molecule is also retrieved by multiplicatively scaling the a priori volume mixing ratio in all layers by a single factor.

[11] Retrievals from the Ny Ålesund and Pasadena locations relied on the "GFIT" software [*Toon et al.*, 1999], also referred to as the "GGG code" by *Goldman et al.* [1999]. The algorithm was adapted from codes initially used for the ATMOS solar occultation geometry [*Norton and Rinsland*, 1991] to allow retrievals of total columns from the ground, including simultaneous fitting of multiple gases. The forward model has 1-km-thick layers extending from the surface to 100 km altitude.

[12] Total columns retrieved with SFIT1, SFIT2, and GFIT have been compared for several molecules (including HCl) and found to agree within their respective error limits of a few percent [*Goldman et al.*, 1999]. A comparison of profile retrievals obtained with SFIT2 and the PROFFIT algorithm adopted for retrievals from the Kiruna spectra is currently in progress. Retrieved column biases of up to a few percent may occur for a variety of reasons, e.g., when estimating the contribution of the troposphere to the total HCl column, which can be potentially significant for sites located near sea level [*Rinsland et al.*, 1991, section 2]. The a priori volume mixing ratios of $ClONO_2$ in the troposphere have been assumed to be negligibly small above all stations.

[13] The analysis of $ClONO_2$ requires special comments because of the difficulty in its retrieval due to the weakness

of its absorption feature at 780.22 cm^{-1}. Moreover, this feature is located in the wing of a strong temperature-sensitive H_2O line at 779.304 cm^{-1} and is overlapped by a temperature-sensitive CO_2 line and several other weaker absorbers [see *Rinsland et al.*, 1996] (Figure 1) for molecule-by-molecule simulations of the target and interfering gas absorptions in this region). Tests have shown the importance of accurately simulating the H_2O and CO_2 absorptions in the $ClONO_2$ region with most sites adopting the "broad window/narrow window" two-step retrieval approach first described by *Reisinger et al.* [1995].

[14] Except for updates to H_2O and HDO spectroscopic parameters based on the work of *Toth* [1998] and the $ClONO_2$ updates described below, most analyses relied on spectroscopic parameters compiled in the 1996 High-resolution Transmission (HITRAN) database [*Rothman et al.*, 1998].

[15] Retrievals of $ClONO_2$ from all sites except Kiruna assumed $ClONO_2$ "pseudolines" derived at the Jet Propulsion Laboratory (JPL) by one of us (G.C.T.) from fits to temperature- and pressure-dependent 0.0009–0.008 cm^{-1} resolution laboratory spectra measured between 190 and 296 K and between 0.3 and 1.0 hPa [*Birk and Wagner*, 2000; M. Birk, private communication, 2001]. Nearly 30 of these laboratory spectra were analyzed with the GFIT algorithm to generate the set of $ClONO_2$ pseudolines by simultaneously fitting transmission spectra reproduced from the laboratory absorption coefficients. The line list was generated solving for the intensity at 296 K and the lower state energy of each pseudoline. The pressure-broadening coefficient of the pseudolines was determined empirically by trying different values and selecting the one that gave the best overall fit. All lines were assumed to have the same air-broadening coefficient at 296 K. The coefficient of the temperature dependence of the air-broadening coefficient was also assumed to be the same for all pseudolines. Laboratory $ClONO_2$ columns derived from fits with these pseudolines agree to within 4% with $ClONO_2$ columns calculated from the laboratory cell conditions with typical deviations of 2% over the 690–1330 cm^{-1} range of the laboratory spectra. The pseudolines also provide improved consistency between $ClONO_2$ amounts retrieved from Mark IV (MkIV) balloon-borne solar occultation spectra measured in the 780–1292 cm^{-1} region. The analysis of $ClONO_2$ from the Kiruna station assumed *Birk and Wagner*'s [2000] temperature-dependent absorption coefficients.

[16] Analyses of atmospheric solar spectra with *Birk and Wagner* [2000] parameters yield improved fits to the $ClONO_2$ ν_4 band Q branch compared to retrievals with previous sets of $ClONO_2$ spectroscopic parameters [*Ballard et al.*, 1988; *Bell et al.*, 1992]. The better fits to atmospheric measurements are primarily a consequence of the full range of atmospheric temperatures and pressures included in *Birk and Wagner*'s [2000] laboratory measurements (*Ballard et al.*'s [1988] measurements were limited to low pressures).

[17] Total $ClONO_2$ columns retrieved from atmospheric spectra with *Birk and Wagner*'s [2000] absorption cross sections are 5–10% lower than those derived with the linelist of *Bell et al.* [1992] and ∼30% lower than obtained with *Ballard et al.*'s [1988] list (T. Blumenstock, private communication, 2001). Biases between total columns retrieved with *Bell et al.* [1992] and *Ballard et al.*'s [1988] pseudoline spectroscopic parameters have been
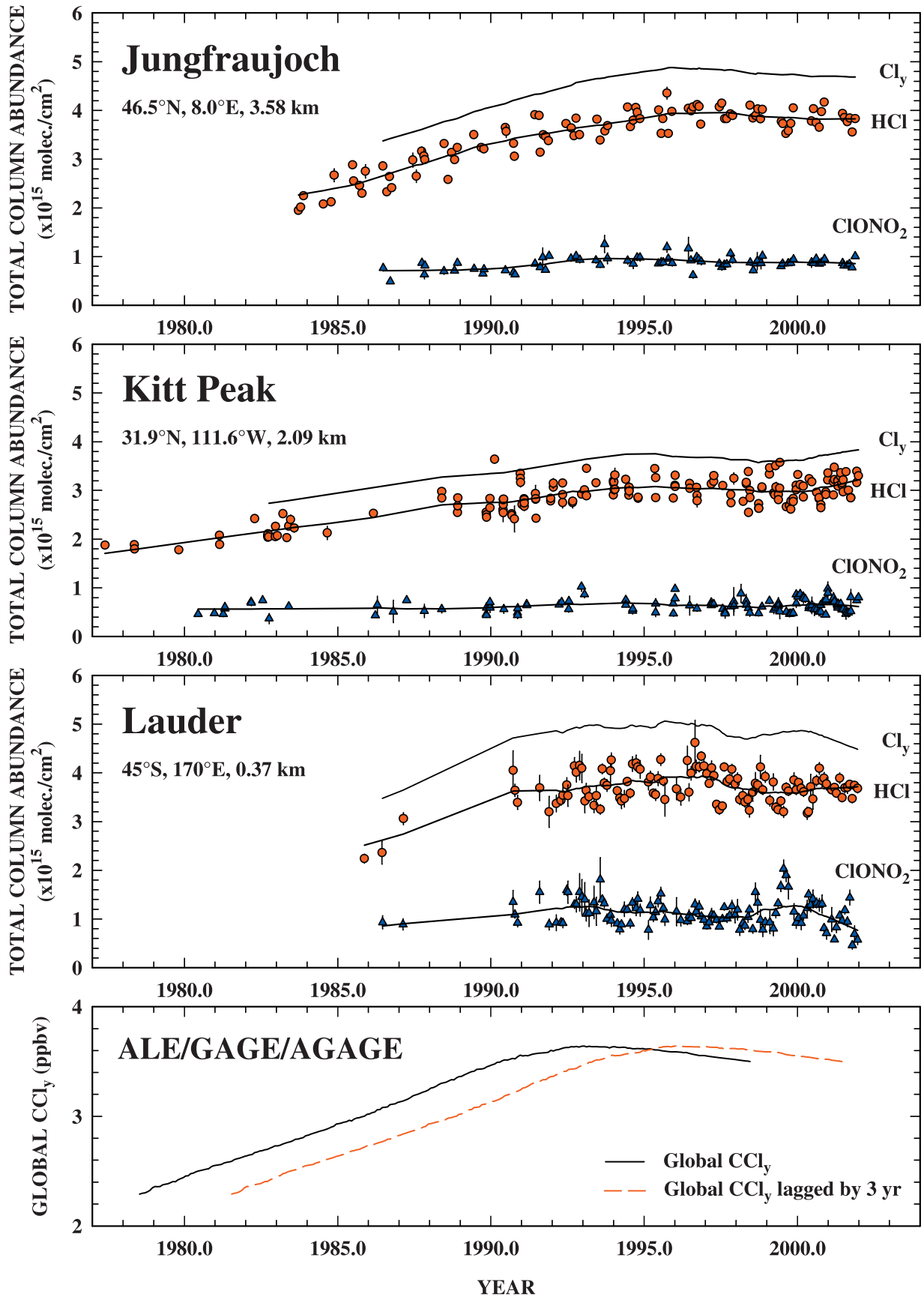
Table 1. Location of the NDSC Sites Involved in This Study, Data Series Investigated, and Retrieval Algorithms Adopted[a]

Station	Latitude	Longitude	Altitude a.s.l., km	HCl Time Span, (Retrieval Algorithm)	ClONO$_2$ Time Span, (Retrieval Algorithm)
Ny Ålesund[b]	78.9°N	11.9°E	0.01 or 0.02	July 1993–Sept. 2001 (GFIT)	July 1993–Sept. 2001 (GFIT)
Kiruna[c]	67.8°N	20.4°E	0.41	June 1996–Nov. 2001 (PROFFIT)	June 1996–Nov. 2001 (PROFFIT)
Zugspitze[c]	47.4°N	11.0°E	2.96	June 1995–Nov. 2001 (SFIT1)	July 1996–Nov. 2001 (SFIT2)
Jungfraujoch[c]	46.5°N	8.0°E	3.58	July 1977–Dec. 2001 (SFIT1)	June 1986–Dec. 2001 (SFIT2)
Pasadena[d]	34.2°N	118.2°W	0.34–3.80	June 1987–Nov. 2001 (GFIT)	Sept. 1994–Nov. 2001 (GFIT)
Kitt Peak	31.9°N	111.6°W	2.09	May 1977–Dec. 2001 (SFIT2)	June 1980–Dec. 2001 (SFIT2)
Mauna Loa[e]	19.5°N	155.7°W	3.40	Nov. 1991–July 1994; Aug. 1995–June 2000, May 2001–Nov. 2001 (SFIT2)	Aug. 1995–March 2000, April 2001–Nov. 2001 (SFIT2)
Wollongong	34.4°S	150.9°E	0.03	June 1995–Oct. 1995; May 1996–Dec. 2001 (SFIT2)	May 1997–Jan. 1998; June 1999–Dec. 2001 (SFIT2)
Lauder	45.0°S	169.7°E	0.37	Nov. 1985–Dec. 2001 (SFIT2)	June 1986–Dec. 2001 (SFIT2)

[a]Full range of solar measurement time periods by month and year.
[b]Only solar measurements between day 140 and day 270 of each year are reported.
[c]Monthly mean measurements between June and November of each year have been included here for the trend determinations.
[d]Includes measurements from six sites between 32°N and 37°N latitude. See section A6.
[e]Spectra were recorded from 1991 to 8/95 with a Bomem interferometer. Subsequently, spectra were recorded with a Bruker interferometer which was inactive during June 2000–April 2001. See section A7.

quantified previously [*Rinsland et al.*, 1996] and discrepancies between modeled and retrieved ATMOS ClONO$_2$ profiles have been reported [*Rinsland et al.*, 1994].

3. Measurements and Analysis

[18] Table 1 gives the locations of the nine NDSC sites, the time span of the total column measurements, and the retrieval algorithms used in the analysis. As indicated in the footnotes for this table, measurements from the four most northerly locations exclude time periods of increased meridional transport, perturbed stratospheric chemistry, and descent when chemical losses of ozone occur due to chlorine and bromine activation [*World Meteorological Organization* (*WMO*), 1999, section 7]. Although chemically processed Antarctic filaments have been observed above the Lauder station during austral winter [*Brinksma et al.*, 1998], their appearance is a rare event, so that the Lauder monthly mean total column abundances for both HCl and ClONO$_2$ have been retained year-round. Analysis of a multiyear time series of FTIR column measurements above Arrival Heights, Antarctica (77.8°S, 166.7°E, 200 m a.s.l.) shows that by the time the vortex breaks up (usually during November or early December), chlorine activation has ended and HCl levels have returned to unperturbed values [*Wood et al.*, 2001].

[19] Details of the measurements and analysis approach at each site are reported in the sections given in Appendix A, beginning with those three with the longest time bases for HCl and ClONO$_2$, i.e., Kitt Peak (USA), Jungfraujoch (Switzerland) and Lauder (New Zealand). Descriptions follow for Ny Ålesund (Spitzbergen), Zugspitze (Germany), Pasadena (USA), Mauna Loa (USA), Wollongong (Australia), and Kiruna (Sweden).

[20] The theoretical altitude sensitivity of a measurement may be directly assessed by examination of its averaging kernels [*Rodgers et al.*, 1990]. The latter show how a total column can be sounded and resolved vertically [*Connor et al.*, 1996], and this can provide some indication about the mean age of the sampled air. As discussed by *Connor et al.* [1996], the kernels depend on the selected target transitions, the a priori assumptions, and constraints adopted to retrieve the column from the spectrum. A perfect measurement would sample the intended region uniformly and not include contributions from outside that region. Sample column averaging kernel calculations for HCl and ClONO$_2$ are presented and discussed in the section A1 of Appendix A. As illustrated in these examples, total column averaging kernels for individual NDSC stations show the HCl and ClONO$_2$ measurements sample the atmosphere with low vertical resolution. Low sensitivity in the troposphere increases to a broad maximum in the lower stratosphere for profile retrievals to a broad maximum in the upper stratosphere for retrieval by multiplicative scaling of the a priori profile in all layers. Comparison of the total column kernels with mean age spectra as a function of altitude and latitude from models and measurements [Figures 7 and 8 of *World Meteorological Organization* (*WMO*), 1999] show the total columns gathered at the three NDSC sites with long temporal data sets sample air containing a range of ages, typically 3–4 years older than air entering the stratosphere through the tropical tropopause.

4. NDSC-Cl$_y$ Total Column Measurement Time Series

[21] As pointed out in section 1, the two most important constituents of relevance to the subject of this investigation

Figure 1. (opposite) The evolution of inorganic chlorine, Cl$_y$, as derived for the three NDSC sites with the longest data sets, ordered north to south by latitude. The Cl$_y$ curves (solid black) were obtained by adding the nonparametric least squares fits to the HCl (red) and ClONO$_2$ (blue) data points (monthly means for Jungfraujoch and Lauder and daily means for Kitt Peak). Error bars correspond to the standard deviations of the daily or monthly means. The black solid curve in the bottom panel displays the total organic chlorine volume mixing ratio (CCl$_y$) measured at the ground by the AGAGE network. The red dashed curve shows the same CCl$_y$ shifted in time by 3 years to approximately account for the time delay for transport of tropospheric air to the altitudes sampled by the ground-based measurements. See section 4 for additional details.

are HCl and ClONO$_2$, which together contribute about 92% of the total loading of inorganic chlorine, Cl$_y$, in the stratosphere under background conditions [*Zander et al.*, 1992]. The total columns of these two constituents monitored at the nine NDSC locations involved here are displayed in Figures 1–3. These figures show that three sites, namely Jungfraujoch, Kitt Peak, and Lauder, currently possess data for both molecules over time periods much longer than the other sites (Ny Ålesund, Kiruna, Zugspitze, Pasadena, Mauna Loa, and Wollongong), though the Pasadena HCl time series extends over 15 years. Total HCl columns from all nine NDSC sites increase with latitude, a result expected from (1) the location of this species primarily in the stratosphere, (2) the decline of the mean tropopause height toward the poles, and (3) the increasing conversion of organic chlorine to Cl$_y$ in the more photochemically aged higher latitude air.

[22] The black Cl$_y$ curves displayed for each location in Figure 1 were obtained by adding the curves fitted to HCl (red circles) and ClONO$_2$ (blue triangles) total column measurements. As noted in Table 1, Jungfraujoch data used here are limited to the June–November monthly mean columns to avoid transport of air masses from polar regions with perturbed lower stratospheric chemistry during winter/spring time periods [*Rinsland et al.*, 1996]. The presence of perturbed conditions above the station due to Arctic air intrusions are readily verified by high HF, high ClONO$_2$, low HCl columns and back-trajectories, and such considerations have been the basis for the selected exclusion period. The Kitt Peak data points are daily averages, while the Lauder ones are monthly means throughout the year. Each fitted curve corresponds to a nonparametric least squares calculation (similar to those described by *Cleveland and Devlin* [1988]), either to the selected daily or monthly averages, and assuming a Gaussian weighting function sampling 20% of the data points.

[23] Overall, the databases from the three long-term sites in Figure 1 show increases in HCl prior to the early 1990s, then progressively reaching a broad plateau extending to the end of the time series. The ClONO$_2$ total columns remain relatively constant until 1991, after which some column enhancements were statistically identified for several years in the nonparametric fits to the Jungfraujoch and Lauder data sets; these are further discussed in section 6, in relation with corresponding model predictions. The resulting Cl$_y$ curves for all three sites reflect primarily the evolution of HCl, which contributes about 75% to total Cl$_y$. The solid curve in the fourth panel of Figure 1 displays the AGAGE time series of global CCl$_y$ measured in situ at the surface [*Prinn et al.*, 2000], while the red dashed curve reproduces the latter time-lagged by 3 years.

[24] Dates of HCl, ClONO$_2$, and Cl$_y$ maxima from nonparametric fits to the three long-term and the Pasadena HCl time series are provided in Table 2. Uncertainty in the date of the maximum Cl$_y$ total columns is about ±2 years with some indication for a second maximum in Cl$_y$ obtained from fits to several time series. Overall, these long-term databases provide evidence that the stratospheric Cl$_y$ rate of increase

progressively slowed during the early 1990s and reached a broad plateau after 1995. Possible natural causes for differences in the maxima include the effects of transport (which mixes air from different latitudes), seasonal and interannual variations, and day-to-day fluctuations in the tropopause height above the sites. The results presented in Figures 2 and 3 from the shorter-term time series of HCl and ClONO$_2$ total columns at the other six NDSC sites are generally consistent with the long-term databases, though the long-term trends are not as well defined because of the shorter time span.
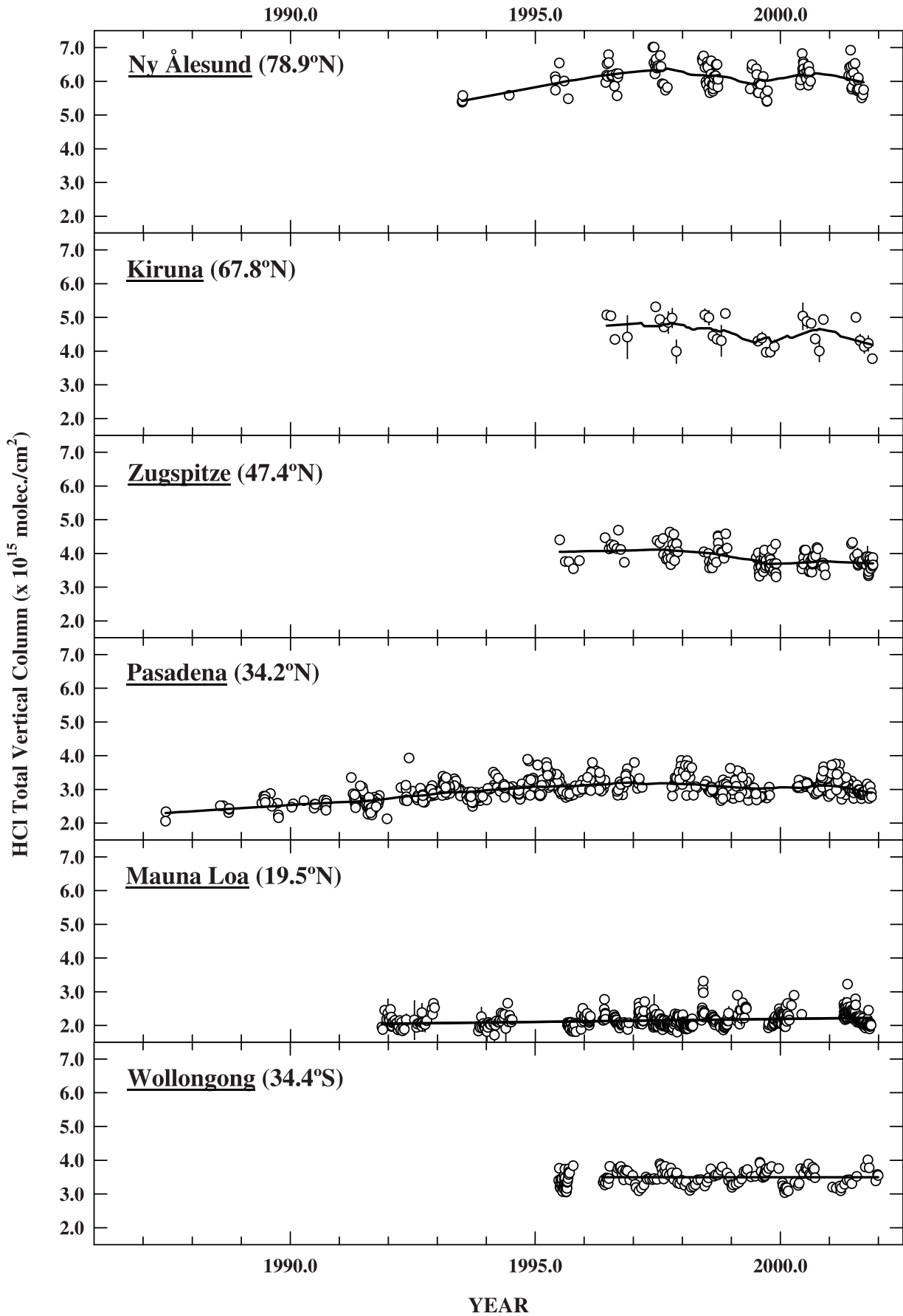
5. Total Chlorine at 55 km From HALOE

[25] Figure 4 presents time series of total chlorine (open circles) at 55 km altitude, based on HALOE-version 19 near-global monthly average measurements of HCl since October 1991, as well as total organic chlorine, CCl$_y$, at the surface based on the Ab baseline scenario (continuous thin curve). The approach for calculating the open circles from individual HALOE retrievals between latitudes of 70°N and 70°S has been described by *Anderson et al.* [2000, section 2]; it derives the total inorganic chlorine loading near the stratopause by applying a latitude-dependent correction to the HCl volume mixing ratio measurements, based on model calculations [*Brasseur et al.*, 1990]. The thick curve is a nonparametric least squares fit [*Cleveland and Devlin*, 1988] to the open circles, with a Gaussian weighting function sampling 15% of the data points. The thin dashed curve represents the surface CCl$_y$ time series lagged by 6 years.

[26] The HALOE-derived time series shows a monotonic increase of the 55-km total chlorine mixing ratio, from about 2.9 ppbv in late 1991 to 3.5 ppbv in mid-1996; within the associated data uncertainties, its subsequent overall behavior can be considered as a leveling off into a broad plateau. The abrupt changes observed in the HALOE data between mid-1996 and 2001 remain unexplained [*Waugh et al.*, 2001; *Engel et al.*, 2002]; they suggest that atmospheric processes other than transport and chemistry partitioning have affected HCl at 55 km altitude [*Randel et al.*, 1999; *Considine et al.*, 1999; *Waugh et al.*, 2001]. The rise following a minimum in mid-1999 indicates a return to consistency with respect to the surface global CCl$_y$ time series assuming the HALOE data, their errors, and a 6-year lag time. The 55-km global average peak, broader than at the surface, is consistent with predictions when considering a narrow "age spectrum" for stratospheric mixing processes [e.g., see Figure 2 of *Waugh et al.*, 2001].

6. Comparison Between Measurements and Model Calculations

[27] Total columns from the three ground-based stations with the longest time spans have been compared with 2-D (latitude-height) dynamical-radiative-chemical model calculations for the closest corresponding latitude grids.

Figure 2. (opposite) Time series of HCl total vertical column abundances measured at six additional NDSC sites, ordered north to south by latitude and fitted versus time as described in section 4. Error bars are standard deviations of the daily or monthly mean as discussed in sections A4–A9.
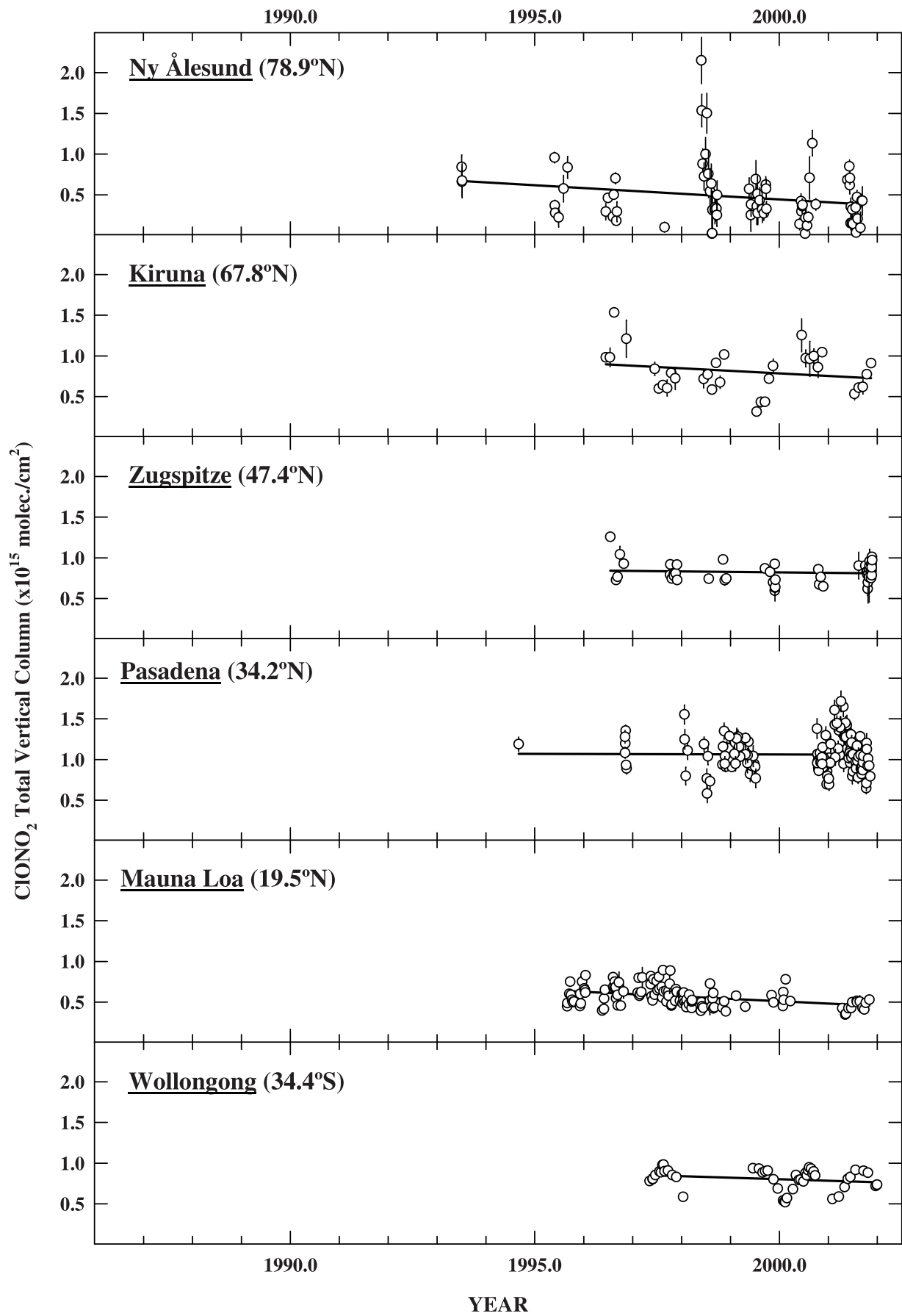
Table 2. Total Column Maxima Obtained for HCl, ClONO$_2$, and Inorganic Chlorine (Cl$_y$) From Nonparametric Least Squares Fits to the Longest NDSC Time Series[a]

Station	Latitude	HCl Peak	ClONO$_2$ Peak	Cl$_y$ Peak
Jungfraujoch	46.5°N	Sept. 1997	Sept. 1993	Dec. 1995
Pasadena	34.2°N	Dec. 1996 Sept. 2000	-	-
Kitt Peak	31.9°N	May 1995 NR	May 1994 June 2000	May 1995 NR
Lauder	45.0°S	Nov. 1996 NR	Oct. 1992 Nov.1999	Sept. 1995 Feb. 2000

[a]See continuous curves fitted to the data points in Figures 1 and 2. NR, second maximum not reached.

The calculations were performed with a 2-D model [*Kinnersley*, 1996] coupled with the chemical module from the SLIMCAT 3-D model [*Chipperfield*, 1999]. The latter module is based on a detailed stratospheric chemistry and CH$_4$ oxidation scheme that incorporates all the species in the O$_x$, NO$_y$, Cl$_y$, Br$_y$, and HO$_x$ families known to be important in stratospheric and CH$_4$ oxidation chemistry. The model also includes longer-lived species such as N$_2$O, CH$_4$, and halocarbons. Heterogeneous chemistry on liquid sulfate aerosols is also applied with aerosol loading specified from zonal mean satellite observations. Aerosol loading was taken from a 1979–1995 climatology [*Jackman et al.*, 1996; *World Meteorological Organization* (*WMO*), 1999] based on measurements from the SAM II, SAGE I, and SAGE II instruments. Time periods before 1979 assume the 1979 loading. After 1995, the model assumes the 1995 aerosol loading, though in reality it has continued to decrease. Parameterization of the three longest Rossby waves is included in the model, which calculates its own temperature field. The 2-D model extends from pole-to-pole with a 9.5° horizontal grid and from the ground to 80 km altitude with ∼3.5 km vertical resolution. The model was integrated from 1970 to 2010 for the present study with time-dependent values of the halocarbons and other source gases specified by past measurements and the "Ab baseline" future scenario developed by Montzka and Fraser [*World Meteorological Organization* (*WMO*), 2003].

[28] The comparison of the monthly average model- and observed total column time series is presented in Figure 5. The model total columns are derived by summing the calculated column amounts in each layer from the site altitudes to the top of the atmosphere. The closest 2-D model grid latitude used here is indicated below each site's coordinates. Measured HCl and ClONO$_2$ total columns are displayed with black open triangles and blue plus symbols, respectively, and the sum of the measured HCl and ClONO$_2$ columns is shown with open red squares (same data as in Figure 1). Corresponding model curves are displayed for HCl (upper black continuous curve), ClONO$_2$ (blue continuous curve), ClO (lower black continuous curve), and HOCl (dashed black curve). A red dashed curve shows the model-predicted sum of HCl and ClONO$_2$ and a red solid curve reproduce model total inorganic chlorine (Cl$_y$). Differences between the fits to the experimental curves of HCl +

ClONO$_2$ and the corresponding model values may in part reflect different a priori assumptions for the tropospheric contributions to the total columns above the stations.

[29] The measured HCl and ClONO$_2$ total columns from all three stations show a near-continuous rise during the 1980s and early 1990s, consistent with the trend in the corresponding model curves. A seasonal variation is superimposed on the model-predicted rise, specific to each station.

[30] The gradual HCl and ClONO$_2$ rises predicted by the model for all three stations are affected by a decrease in column HCl and an increase in column ClONO$_2$ for about 2 years after the massive June 1991 eruption of the Mt. Pinatubo volcano in the Philippine Islands. The changes are caused by an increase in the heterogeneous processing of these species on the elevated aerosol loading in the lower stratosphere. This processing initially produces active chlorine (ClO$_x$), which is then deactivated to form ClONO$_2$. Conversion of chlorine species back to HCl takes place on a longer timescale [*Douglass et al.*, 1995]. Therefore the net effect of increased heterogeneous processing is an increase in ClONO$_2$ [e.g., *Koike et al.*, 1994]. The model-predicted enhancement in ClONO$_2$ during June 1991–December 1992 is apparent in the Lauder observations, and there is also evidence for a post-Mt. Pinatubo eruption ClONO$_2$ enhancement and a correspondingly slower HCl increase in the Jungfraujoch observations (see Figure 1). Despite a limited number of data points between 1991 and 1993, the nonparametric fit detects a slight increase in the Kitt Peak ClONO$_2$ database, commensurate with the weaker model predictions for that site. Other model calculations with standard heterogeneous chemistry predict only small changes in HCl/Cl$_y$ in the nonpolar lower stratosphere even at high aerosol loadings [*Rinsland et al.*, 1994] (Figures 2 and 3). However, recent studies [*Michelsen et al.*, 1999; *Webster et al.*, 2000] have suggested that aerosol-mediated reactions above 200 K are significant and result in repartition of lower stratospheric chlorine after major volcanic eruptions. Enhancements in ClONO$_2$ are also observed later in the time series (e.g., in 1999 at Lauder). These may be linked to transport of ClONO$_2$-rich air from the edge of the winter polar vortex. The 2-D model does not capture this transport. It is to be noted that similar ClONO$_2$ enhancements have also been observed at northern midlatitude sites during winter-spring time [e.g., *Zander et al.*, 1998; *Mahieu*

Figure 3. (opposite) Time series of ClONO$_2$ total columns from six NDSC sites with shorter time periods of measurements, ordered north to south by latitude. Error bars are standard deviations of daily or monthly means as discussed in sections A4–A9.
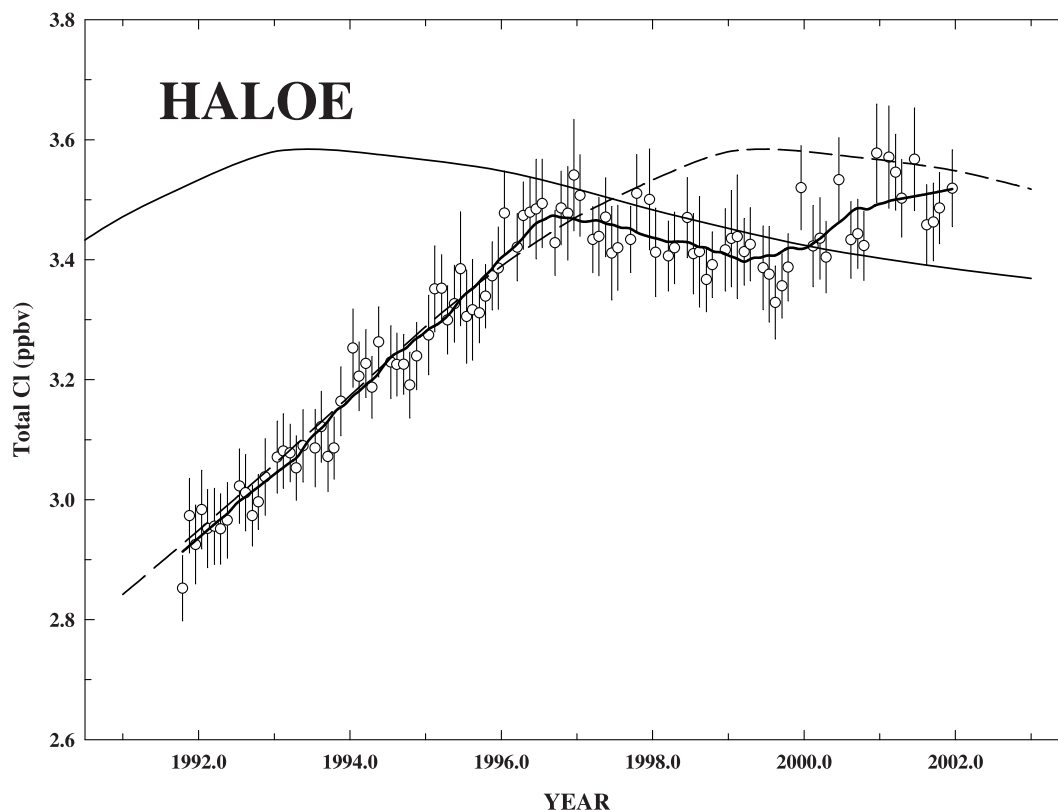
Figure 4. Monthly mean total chlorine volume-mixing ratio time series (open circles) derived from HALOE-version 19 measurements of HCl at a geometric altitude of 55±1km between October 1991 and December 2001. Vertical error bars are 1-σ standard deviations. The thick continuous curve is a nonparametric least squares fit to the open circles. The thin continuous curve represents the temporal evolution of total organic chlorine at the surface (based on the "Ab baseline" emission scenario [*World Meteorological Organization* (*WMO*), 2003]) while the thin dashed curve reproduces the latter lagged by 6 years. For details, see section 5.

et al., 2000; *Sussmann and Wimmer*, 2000], but these have been omitted here by only retaining the summer-fall data sets, to better appraise the long-term changes of prime relevance in this work.
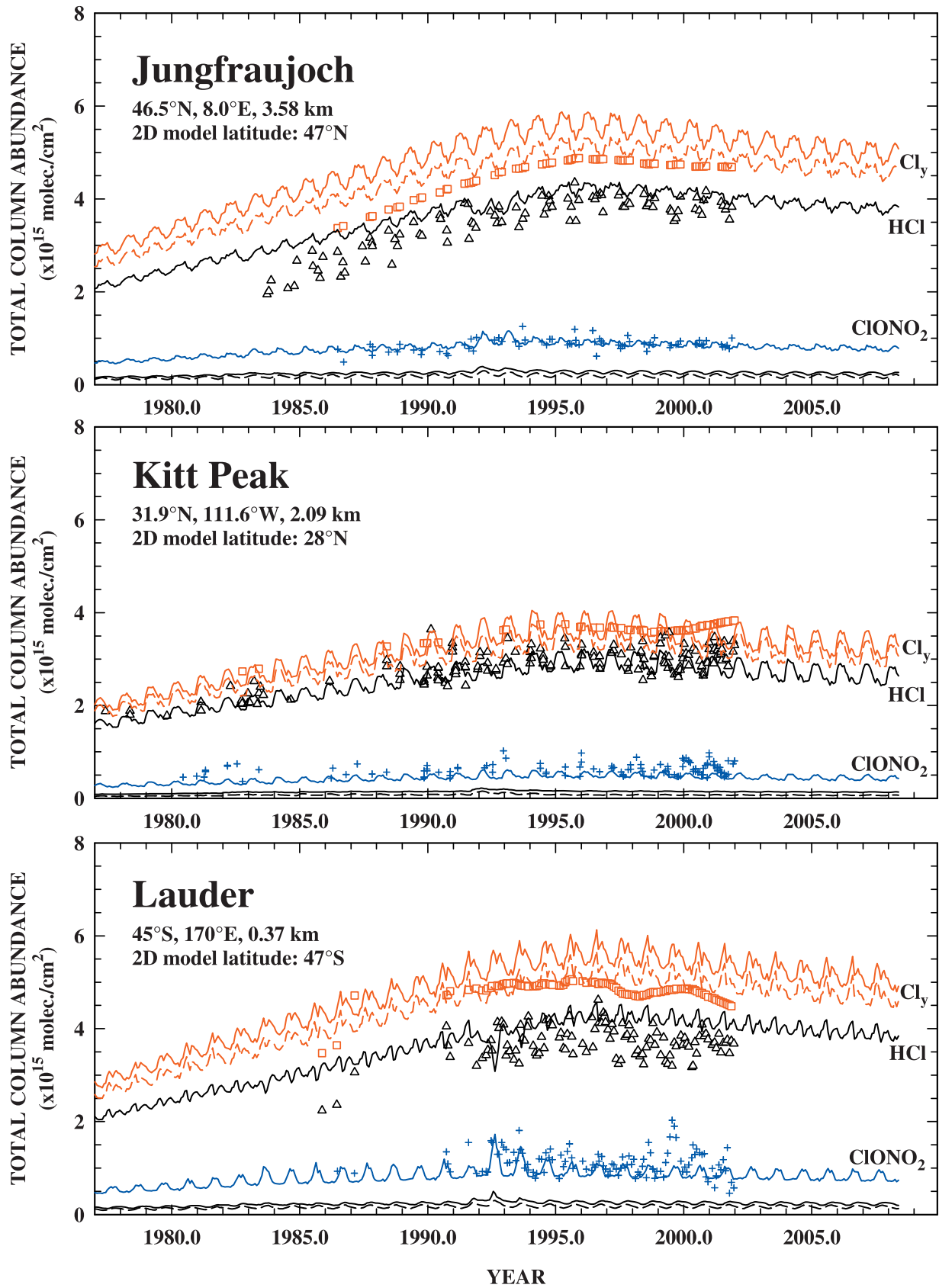
[31] The buildup in the measured and model column time series subsequently slows, with both reaching a broad plateau, followed by a predicted slow decline. The model-predicted maxima in the HCl and ClONO$_2$ total columns above the three stations occur between 1994 and 1996. Seasonal and interannual changes have an important impact on the time of the predicted total column maxima, as the maximum in the total column remains above the largest minimum in the seasonal cycle for around 10 subsequent years. Referenced to the maxima in the seasonal cycle, total

column HCl and ClONO$_2$ loadings above the three stations are predicted to decline by 9–11% in 2006 and by 12–14% in 2010.

7. Summary and Conclusions

[32] Total column abundances of HCl and ClONO$_2$, the primary components of the Cl$_y$ stratospheric inorganic chlorine budget, have been retrieved from ground-based, high-resolution infrared solar spectra recorded over time periods as long as 24 years. Related measurements were made at nine primary or complementary NDSC sites located at latitudes between 78.9°N and 45.0°S. Based on the long temporal databases from Jungfraujoch, Kitt Peak, and

Figure 5. (opposite) Comparison between Cl$_y$ time series derived from observations at the three NDSC sites with the longest records and from two-dimensional (2-D) model calculations. The 2-D model assumes the Ab baseline scenario (S. Montzka and P. Fraser, private communication, 2002), and its monthly average outputs for the closest latitudinal grid points to the stations (indicated on each panel) are displayed. Reproduced for each site are the measured HCl (black open triangles) and ClONO$_2$ (blue plus symbols) columns, as well as the sums of their nonparametric least squares fitted curves from Figure 1 (red squares). Model time series are displayed for HCl (black curve), ClONO$_2$ (blue curve), ClO (black solid curve), and HOCl (black dashed curve), HCl + ClONO$_2$ (red dashed curve), and total inorganic chlorine (Cl$_y$) (red solid curve).

Lauder, the HCl and $ClONO_2$ column sums (which are good surrogates of Cl_y at low latitudes and midlatitudes) show a rapid buildup until the early 1990s, followed by a progressive stabilization into a broad plateau from the mid-1990s through the end of the time series (see Figure 1). These post-1995 results are generally supported by shorter-term databases gathered at six additional NDSC sites (Ny Ålesund, Kiruna, Zugspitze, Pasadena, Mauna Loa, and Wollongong; see Figures 2 and 3). The evidence for stabilization of the inorganic chlorine loading in the stratosphere reported here is consistent with near-global average HALOE concentration measurements of HCl near the stratopause (54−56 km), which also show a rapid increase prior to 1997, followed by a broad plateau. While a maximum in the total inorganic chlorine loading appears to have been reached at the two midlatitude sites of Jungfraujoch and Lauder [RZ1], its time of occurrence remains uncertain to about ±2 years, because of the slow rate of change in the loading and local variability. The mean maximum at the three long-term sites agrees with the time of the peak tropospheric organic chlorine loading which occurred between 1992 and 1994 and model-predicted age distributions [*World Meteorological Organization* (*WMO*), 1999], when taking into account a time delay of about 3−4 years for transport of source gases from the surface to the mean stratosphere sampled here.

[33] The 2-D model calculations specifically performed here also predict a broad maximum, consistent with the measured time series. A slow decline in total Cl_y loading, calculated to have started during the second part of the 1990s and to reach 12−14% in 2010 relative to the maximum, is further predicted when considering the Ab baseline emission scenario of halogenated source gases with large ODPs [*World Meteorological Organization* (*WMO*), 2003].

Appendix A

A1. Kitt Peak (31.9°N, 111.6°W, 2.09 km a.s.l.)

[34] Measurements of HCl and $ClONO_2$ from Kitt Peak are recorded with the 1-m FTS [*Brault*, 1978] in the U.S. National Solar Observatory (NSO) facility. The resolution of individual spectra ranges from 0.005 to 0.019 cm^{-1}, where resolution is defined as $1/2\Delta_{max}$ and Δ_{max} is the maximum optical path difference (OPD). The number of days per year with HCl and $ClONO_2$ measurements range from 1 to 14 and 1 to 18, respectively. The earliest HCl and $ClONO_2$ measurement meeting objective quality criteria were obtained in May 1977 and in June 1980, respectively.

[35] Retrievals of HCl and $ClONO_2$ were both performed with SFIT2 simultaneously fitting the microwindows listed in Table 3. Signal-to-noise ratios of 500 for $ClONO_2$ and 250 for HCl were assumed to provide stratospheric column averaging kernels with maxima close to the same altitude.

[36] The HCl a priori mixing ratio profile for altitudes between 5.5 and 65 km altitude was computed from averages of HALOE-version 19 profiles measured between October 1991 and June 2000 within 5° latitude of the station. Based on the measurements, the assumed a priori profile, and an annual mean tropopause height of 14 km [*Rinsland et al.*, 1998], we estimate the tropospheric HCl column to be equal to 16% of the total.

Table 3. Spectral Regions and Principal Interferences for Kitt Peak Retrieval With SFIT2[a]

Window, cm^{-1}	Species
HCl Retrievals	
2727.74−2727.82	
2775.72−2775.80	CH_4, N_2O, O_3
2925.80−2926.00	CH_4, NO_2, O_3
ClONO₂ Retrievals	
779.05−779.90	H_2O, CO_2, O_3
780.15−780.70	CO_2, O_3, HNO_3
780.90−781.00	CO_2, HNO_3

[a]Vertical profiles of both $ClONO_2$ and H_2O were retrieved. The other species listed in the table were fitted by multiplictative scaling the a priori mixing ratio in all atmospheric layers by a single value. These additional parameters were retrieved as part of the simultaneous analysis of the three microwindows.

[37] The covariance matrix was assumed diagonal with the mixing-ratio uncertainty assumed equal to 1.0 above 11 km and decreasing to 0.5 in the lowermost layer (2.09−3 km). Daily mean National Centers for Environmental Prediction (NCEP) temperature profiles were assumed in the retrievals.

[38] The first panel of Figure 6 displays HCl column-averaging kernels calculated for Kitt Peak with SFIT2, considering the parameter selections and microwindows noted above. Sensitivity is poor in the troposphere, but the stratosphere (located on average at 14 km altitude) is sampled with good sensitivity and nearly uniformly.

[39] The $ClONO_2$ a priori profile was adopted from ATMOS version 3 measurements of the SS72 occultation at 31.5°N latitude during the November 1994 mission [*Irion et al.*, 2002], with a smoothed extension above 38 km and to mixing ratios decreasing to 10^{-12} ppv at 12.5 km and 10^{-13} ppv below 10 km. Profiles of $ClONO_2$ and H_2O were both retrieved. Additionally, CO_2, O_3, and HNO_3 were fitted by multiplicative scaling the a priori profile of each molecule by a single factor. The higher wave number window (see Table 3) provides measurements of CO_2 lines with lower state energies close to that of the CO_2 line interfering with the $ClONO_2$ Q branch. Column averaging kernels for $ClONO_2$ are presented in the second panel of Figure 6. The stratospheric column kernel (14−50 km) shows a broad maximum in the lower stratosphere. The $ClONO_2$ total (2.09−100 km) and stratospheric (14−50 km) column averaging kernels are nearly identical. Peaks of the HCl and $ClONO_2$ 14−50 km averaging kernels occur at 25 and 24 km, respectively.

[40] Figure 7 presents a sample fit to illustrate the consistency obtained from the three HCl microwindows. Error budget calculations performed similarly to those in previous studies [e.g., *Rinsland et al.*, 1991, 1998] indicate that the total random error for a single 14−50 km stratospheric column measurement (arising from temperature profile errors, instrumental noise, and interfering absorption) is 3%. The total systematic error (due to spectroscopic parameter uncertainties, contribution of the a priori profile to the retrieval, forward model approximations, instrument line shape function uncertainties) is estimated to be 5%. Total column random and systematic errors for a single measurement increase to 4 and 8%, respectively. The total column uncertainty increases due to the reduced sensitivity of the
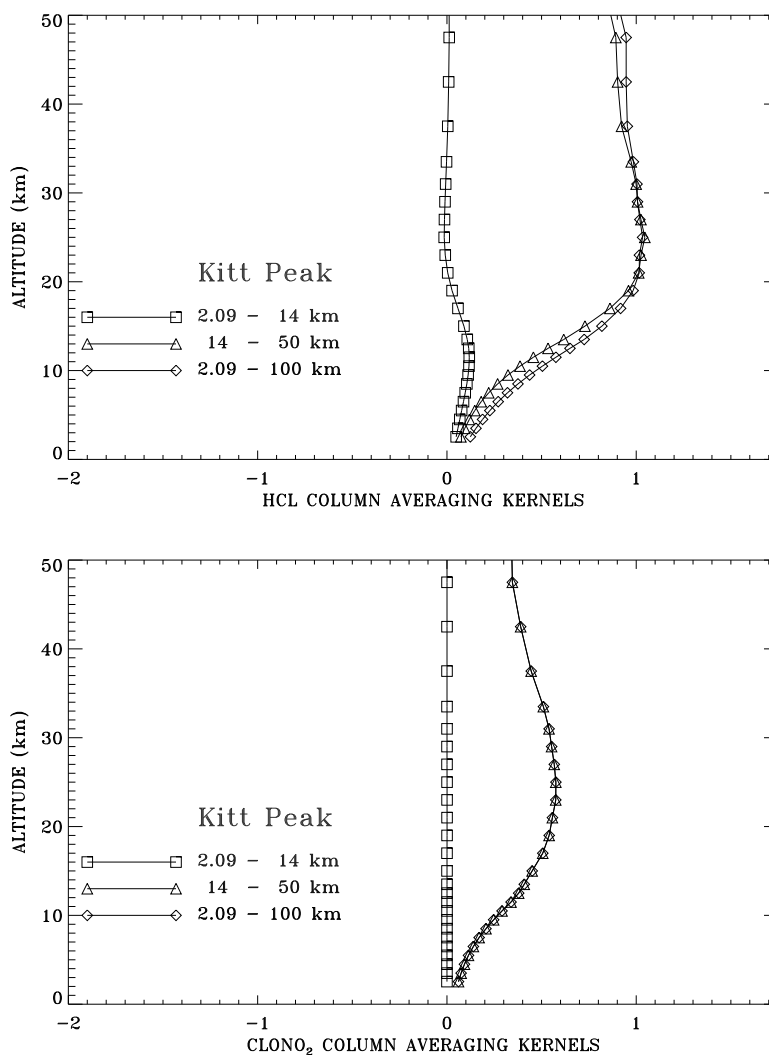
Figure 6. Column averaging kernels for HCl (first panel) and ClONO$_2$ (second panel) above Kitt Peak versus altitude for merged layers corresponding approximately to the tropospheric, stratospheric, and the total column.

measurements below the tropopause, as indicated by the averaging kernels.

[41] A sample fit in the three selected microwindows fitted to derive the ClONO$_2$ profile is presented in Figure 8. The most important atmospheric features are marked and identified. Random and systematic errors for ClONO$_2$ single measurements of the total column are estimated as 9 and 13%, respectively.

A2. Jungfraujoch (46.5°N, 8.0°E, 3.58 km a.s.l.)

[42] The measurements of relevance for this investigation have been obtained primarily with two FTIR spectrometers, i.e., a homemade instrument which began consistent operation in 1985, and a commercial Bruker model 120-HR, installed in 1990. High-quality solar observations have averaged about 50 days per year between 1985 and 1990, increasing to a yearly average of 103 days afterward.

[43] Solar spectra were recorded at resolutions ranging from 0.003 to 0.006 cm^{-1} resolution (resolution defined as in section A1). Most spectra considered here have signal-to-noise ratios ranging from 1500 to 4000 for HCl and from 750 to 3000 for ClONO$_2$. Additional details of the IR instrumentation and measurement procedures have been reported previously [*Zander et al.*, 1993a, 1998; *Mahieu et al.*, 1997; *Rinsland et al.*, 2000a, sections 2 and 4.5]. Vertical column abundances of HCl were derived from solar observations made with a double-pass grating instrument prior to 1985 [*Zander et al.*, 1987]; the consistency of the columns derived from both the latter and the FTIR instruments has been verified from intercomparisons conducted between 1985 and 1989.

[44] The daily mean pressure-temperature profiles adopted in the analysis were provided by the NCEP. The lower-altitude profiles were smoothly connected to *Committee on Extension of the U. S. Standard Atmosphere* (*COESTA*) [1976] profiles above 55 km.

[45] HCl total columns were retrieved with SFIT1 using a single window (2925.74–2926.06 cm^{-1}) encompassing the R(1) HCl line. The a priori HCl profile was derived from ATMOS Spacelab 3 measurements at 30°N [*Zander et al.*, 1992], smoothly connected to a standard reference profile
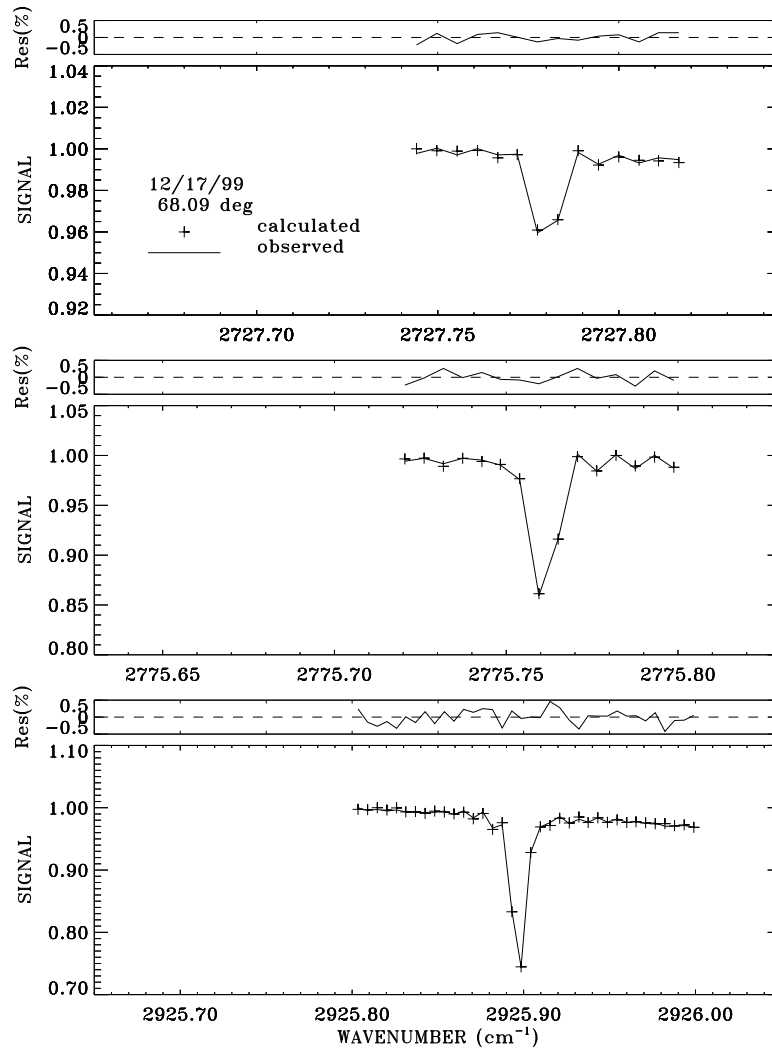
Figure 7. Sample Kitt Peak observed and fitted microwindows encompassing the R1, P5, and P7 HCl lines used for column retrievals. The astronomical zenith angle of the observation is indicated. Residuals (measured minus calculated values) are shown above each spectral plot on an expanded vertical scale.

below the tropopause. Spectroscopic parameters adopted for the HCl analysis were taken from the HITRAN 1991/1992 editions [*Rothman et al.*, 1992]. Typical random and systematic errors of a single HCl column measurement are estimated to be ±3 and ±5%, respectively. As many as 32 individual measurements have been used to produce daily means with random errors reduced accordingly. Monthly mean HCl columns averaged 5 days of observation prior to 1991 and 7 days thereafter.

[46] Retrievals of $ClONO_2$ columns were performed using SFIT2, with an a priori profile from a November 1994 ATMOS version 3 retrieval [*Irion et al.*, 2002] at 45°N latitude and 6°E longitude. The two-step sequential wide/narrow microwindow retrieval approach [*Reisinger et al.*, 1995] was implemented for use with SFIT2. A broad region (from 779.3 to 780.6 cm^{-1}) was first fitted to retrieve H_2O, CO_2, and O_3. Subsequently, the profiles of H_2O and CO_2 were held fixed in the next step to retrieve the profiles of both $ClONO_2$ and O_3 in the narrower 780.05–780.355 cm^{-1} microwindow. As both HNO_3 and COF_2 absorb

weakly in the narrow interval, they were also fitted by multiplicatively scaling their a priori profiles.

[47] Random and systematic errors for a single $ClONO_2$ column measurement have been estimated at ±10 and ±15%, respectively, when using the improved pseudolines based on the work of *Birk and Wagner* [2000] (see section 2).

A3. Lauder (45.0°S, 169.7°W, 370 m a.s.l.)

[48] Infrared solar absorption spectra were first recorded from the Lauder NDSC station in 1985, 1986, and 1987 on a campaign-type basis at 0.02-cm^{-1} resolution with a Bomem FTIR [*Murcray et al.*, 1989; *Matthews et al.*, 1989]. The measurements covered 3–5 and 8–12 µm. The early Bomem HCl and $ClONO_2$ measurements have been recovered and are included in the present analysis. Regular high-spectral resolution measurements began in September 1990, first with a Bruker 120-HR, which was replaced in September 1992 with a Bruker 120-M. All three time series have been analyzed with SFIT2, first for daily means, then averaged to create monthly means, providing a 16-year time span for HCl
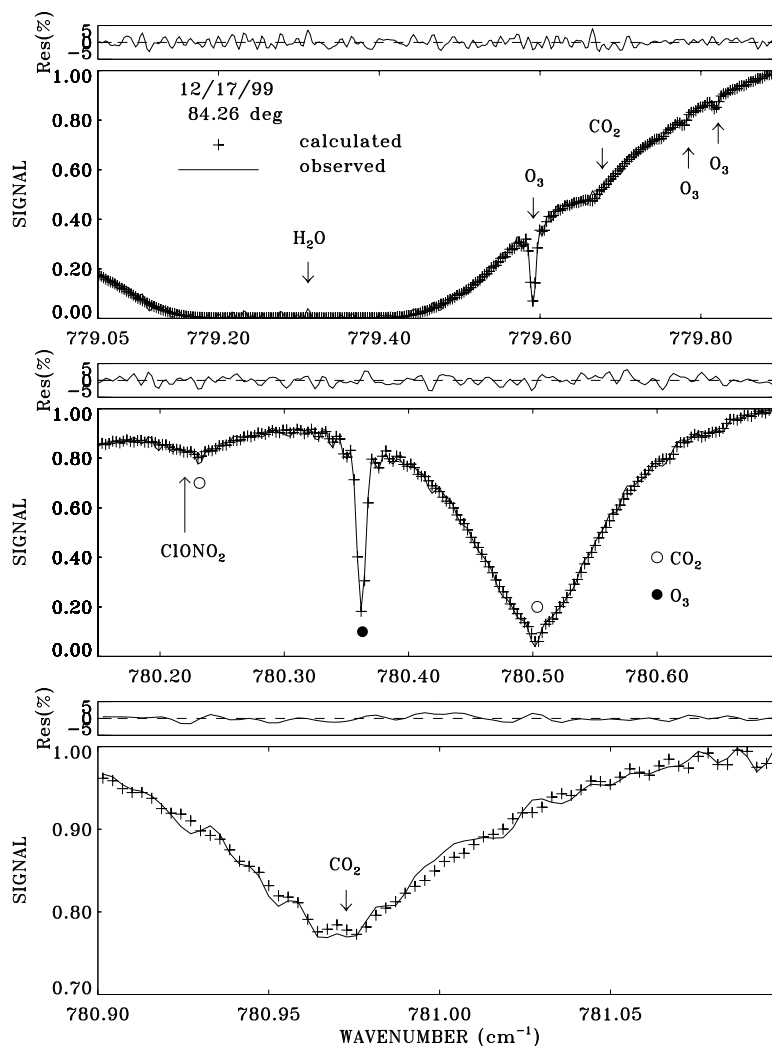
Figure 8. Sample Kitt Peak microwindows simultaneously fitted for deriving the $ClONO_2$ columns above the site, based on the ν_4 band Q branch at 780.22 cm^{-1}, are displayed in the same format as Figure 7. The strongest absorption lines of H_2O, CO_2, and O_3 as well as the $ClONO_2$ feature are marked.

(November 1985–December 2001) and a 15-year-time span for $ClONO_2$ (June 1986–December 2001). Typically, 12 spectra were recorded for both molecules during each month.

[49] Retrievals of HCl were performed by fitting the 2925.9-cm^{-1} R(1) line only (see Table 3) from spectra generated from truncated interferograms transformed with a triangular apodization function. The corresponding spectral resolution is 0.02 cm^{-1} (OPD 50 cm). The early Bomem spectra were analyzed assuming a signal-to-noise ratio of 300:1. Spectra recorded from 1990 onward were analyzed assuming a signal-to-noise of 1000:1. The covariance matrix was assumed diagonal with a relative uncertainty of 0.5 in each layer with the HCl a priori mixing ratio profile between 8 and 65 km altitude computed from averages of HALOE version 19 profiles measured from October 1991 to June 2000 within 5° latitude of the station. Total columns from individual spectra are estimated to have a precision of ±10%, corresponding to ±4% after monthly averaging.

[50] The $ClONO_2$ retrievals were also performed from spectra reduced to 0.02-cm^{-1} resolution to improve the signal-to-noise ratio. The modified version of the two-step wide/narrow microwindow retrieval method [*Reisinger et al.*, 1995] adopted for the Jungfraujoch analysis was used in combination with the pseudolines described in section 2. The $ClONO_2$ a priori profile from ATMOS version 3 measurements [*Irion et al.*, 2002] from March 1992 at 45°S latitude was adopted and smoothly connected to a standard reference file above the range of the ATMOS measurements and to negligibly small mixing ratios below the tropopause. Individual $ClONO_2$ total columns have an estimated precision of 25% [*Reisinger et al.*, 1995], corresponding to about ±4% uncertainty after monthly averaging. Column averaging kernels for Lauder HCl and $ClONO_2$ are similar to those in Figure 6, with peaks in the lower stratosphere for both molecules.

A4. Ny Ålesund (78.9°N, 11.9°E, 10/20 m a.s.l.)

[51] Solar spectra can be recorded from the NDSC primary station in Spitzbergen between mid-March and mid-October and were recorded unapodized with a Bruker 120M FTS [*Notholt*, 1994] from March 1992 until June

1995. The instrument achieved a maximum OPD of 256 cm corresponding to a spectral resolution of 0.0035 cm^{-1} [*Notholt and Schrems*, 1995]. Since that time, measurements have been recorded with a Bruker 120-HR FTS capable of a maximum OPD of 360 cm. In November 1994, the FTS was moved 200 m from its initial location at 10 m a.s.l. to a new NDSC building, 20 m a.s.l. Broadband filters limit the wavelength coverage to increase the signal-to-noise ratio in both the HCl and ClONO$_2$ absorption regions. Daily balloonsonde temperature/pressure profiles measured above the site were adopted up to about 30 km; they were extended to higher altitudes assuming a subarctic temperature profile [*Notholt et al.*, 1995].

[52] Column abundance of both HCl and ClONO$_2$ were retrieved with the GFIT software [*Notholt et al.*, 1997a, 1997b; *Toon et al.*, 1999]. The technique uses nonlinear least squares fitting with compression of the vertical profile above the tropopause for each species to account for subsidence. Initial volume mixing ratio profiles for retrievals and corrections for interfering absorptions were based on midlatitude balloon data [*Peterson and Margitan*, 1995], except for H$_2$O.

[53] Total HCl columns for each observation were calculated by combining the results retrieved separately from three microwindows in the HCl (1-0) band [see Table 1 of *Notholt et al.*, 1997b]. The ClONO$_2$ total columns were retrieved from fits to the ν_4 band Q branch at 780.22 cm^{-1} [see Table 1 of *Notholt et al.*, 1997b] with a 2-cm^{-1} wide microwindow. Daily average total columns were calculated from typically six solar spectra.

A5. Zugspitze (47.4°N, 11.0°E, 2.96 km a.s.l.)

[54] Infrared solar spectra of HCl and ClONO$_2$ have been recorded from the summit of the Zugspitze, Germany, with a Bruker model 120 HR spectrometer. The NDSC primary instrument is operated year-round under full remote control for both atmospheric chemistry and satellite data product validation studies.

[55] All HCl spectra analyzed here were recorded with a maximum OPD of 175 cm (0.0052-cm^{-1} resolution, defined as 0.9 divided by the maximum OPD) [*Sussmann and Schäfer*, 1997; *Sussmann*, 1999; *Sussmann and Wimmer*, 2000]. Most of the ClONO$_2$ observations were recorded with a maximum OPD of 250 cm (0.0036-cm^{-1} resolution). Typically, five measurements were averaged to achieve signal-to-noise ratios of 1000 for HCl and of 250–300 for ClONO$_2$. Temperature profiles assumed in the analysis were based on correlative radiosonde measurements from the station "Munich" of the German Weather Service, located 80 km north of the Zugspitze, and smoothly connected to the *U.S. Standard Atmosphere* [1976] above the highest altitude of the soundings.

[56] Zugspitze retrievals of HCl and ClONO$_2$ were run with the SFIT1 and SFIT2 algorithms, respectively. The a priori profile for HCl was the same as that adopted for the Jungfraujoch analysis; it was multiplicatively scaled and vertically shifted around the tropopause level, stretching or compressing the profile above and below, to account for vertical tropopause displacements and achieve a good fit to the absorption features [*Sussmann and Wimmer*, 2000]. Line parameters for analysis of the R(1) HCl line

were adopted from the 1996 HITRAN compilation [*Rothman et al.*, 1998]. The ClONO$_2$ a priori profile adopted at Zugspitze has been constructed using volume mixing ratios of for levels between 0 and 12 km altitude, a linear interpolation of ATMOS original data [*Irion et al.*, 2002] to levels between 12.5 and 31.5 km, and a standard profile between 32 and 100 km. The two-step retrieval method [*Reisinger et al.*, 1995; *Rinsland et al.*, 1996] and the pseudolines described in section 2 were used.

A6. Pasadena (34.2°N, 118.2°W, 350 m a.s.l.)

[57] Solar absorption measurements of HCl and ClONO$_2$ were obtained with the MkIV Fourier transform spectrometer [*Toon*, 1991], which records the 650–5650 cm^{-1} domain at once with parallel InSb and HgCdTe detectors. Unapodized spectra derived from 116-cm maximum OPD interferograms have been analyzed. Field of view diameters were 3.6 mrad in the InSb and 4.3 mrad in the HgCdTe regions, respectively. Typically, four to six interferograms were averaged to achieve signal-to-noise ratios of 600:1 both in the HCl and ClONO$_2$ regions. Corrections for detector nonlinearity were applied to the HgCdTe measurements [*Abrams et al.*, 1994]. Zero-level offsets were less than 1% as determined from measurements in regions containing saturated spectral lines (e.g., H$_2$O). Measurements span June 1987 to October 2001 with daily averages computed from typically four measurements per day.

[58] Although most of the spectra were recorded from the JPL site, measurements from seven different locations between 32°N and 37°N latitude were included to extend the coverage, with most recent observations recorded from Mt. Barcroft (37°N, 118°W, 3.80 km altitude). Additional MkIV ground-based data sets were included from Ft. Sumner and Daggett (both at 34°N) while waiting for balloon flights from NASA, Ames (37°N), from Palestine, TX (32°N), and from the Table Mountain Facility (34°N) to provide more complete sampling of the seasonal cycle than the JPL data alone.

[59] To minimize the small biases between the different sites arising from their different latitudes and altitudes, and hence align them to JPL conditions, two small corrections have been applied to the raw HCl columns: (1) a 2%/degree latitude gradient was applied to the non-JPL sites, reducing the Barcroft columns (37°N) by 6%, and (2) the measured column amounts were corrected to sea level by assuming a 10 pptv (1 pptv = 10^{-12} per unit volume) HCl mixing ratio below 4 km altitude. This amounts to a correction of $+0.07 \times 10^{15}$ mol cm^{-2} (+2%) for the Barcroft observations. Overall, the raw Barcroft columns have been changed by $-6 \pm 2\%$.

[60] Total ClONO$_2$ columns were retrieved from a single microwindow covering 779.68–781.76 cm^{-1} and fitting for O$_3$, CO$_2$, H$_2$O, and C$_2$H$_2$ in addition to ClONO$_2$. Although the measurements from the high-altitude stations at Mt. Barcroft and Table Mountain are of high quality, they span only the last 3 years, and have not been used to derive a trend. The lower-altitude ClONO$_2$ measurements are also not suitable for deriving a reliable trend due to their low air mass (due to the presence of tall buildings at JPL) and the lack of auxiliary information concerning the profiles of temperature, H$_2$O,

and CO_2, which strongly influence the $ClONO_2$ retrievals under low-altitude conditions.

A7. Mauna Loa (19.5°N, 155.7°W, 3.40 km a.s.l.)

[61] Most of the Mauna Loa measurements included in this study were obtained with a Bruker 120-HR FTIR. The highly automated and computer-controlled observing system has been described previously [*Rinsland et al.*, 1999, section 2]. Measurements of HCl with this system began in August 1995 and extended through November 2001. Early infrared spectra recorded with an FTIR at 0.02 cm^{-1} resolution on 4 days in February 1987 were analyzed to derive HCl total columns [*Rinsland et al.*, 1988]. Observations were also recorded between November 1991 and August 1995 with a Bomem model DS3.002 FTS operating typically at 0.005 cm^{-1} spectral resolution; these latter measurements are also included in the present database.

[62] The Mauna Loa HCl retrievals were obtained with SFIT2 assuming the same line parameters and microwindows as adopted for Kitt Peak (except for the Bomem observations which cover only the R1 line), with a signal-to-noise ratio of 500, consistent with the quality of typical observations. A priori mixing ratio profiles were selected from HALOE measurements with the same criteria as described for Kitt Peak. The HCl covariance matrix was assumed diagonal with a constant relative uncertainty of 1.0 adopted for all layers. Temperature profiles from correlative NCEP measurements were assumed in the analysis.

[63] Profiles of $ClONO_2$ were retrieved from coadded spectra generated for $775-785$ cm^{-1}. Spectra (obtained by the Bruker system) recorded over a solar zenith angle range of up to $1°$ were included from typically three to eight spectra. A zero-level shift was applied based on measurements of fully saturated absorptions in the interval. The a priori vertical distribution was adopted from ATMOS occultation SS89 recorded near the same latitude during November 1994 [*Irion et al.*, 2002] with extensions to both lower and higher altitudes. A signal-to-noise ratio of 500 was assumed, consistent with the noise level in typical spectra.

A8. Wollongong, Australia (34.45°S, 150.88°E, 30 m a.s.l.)

[64] The infrared solar absorption spectra were initially recorded with a Bomem model DA-3 FTS at 0.02-cm^{-1} resolution (50 cm OPD) beginning in June 1995. The instrument was replaced with a Bomem DA-8 in May 1996 and used at 0.004-cm^{-1} resolution (250 cm OPD) [*Griffith et al.*, 1998]. The site is on the University of Wollongong campus on the Australian east coast. Spectra are recorded unapodized with either an HgCdTe or InSb detector in combination with band-pass optical filters covering intervals $400-1000$ cm^{-1} wide. Measurements of $ClONO_2$ have been markedly improved since August 1999 by the use of narrower optical filters covering the region below 1000 cm^{-1}. Additional observational details have been reported previously [*Griffith et al.*, 1998; *Rinsland et al.*, 2001].

[65] Temperature-pressure-altitude-humidity profiles were based on radiosondes launched daily from the Sydney Kingsford-Smith airport, 56 km north of the Wollongong site. Above the maximum sounding altitude (typically 25 km), pressures and temperatures were spline fitted into daily satellite-derived profiles from NCEP.

[66] Retrievals were performed with SFIT2 and a 39-layer model atmosphere. The stratospheric portion of the HCl a priori volume mixing ratio profile was obtained from an interpolation of an average of more than 6 years of version 19 monthly mean HALOE profiles between 32°S and 36°S latitude and 0.46–100 hPa ($\sim$16–51 km), interpolated to the latitude of Wollongong. For altitudes not covered by HALOE observations we based our a priori profile for HCl and interfering species on MKIV solar occultation profiles measured at 34.0°N latitude 109.4°W longitude during a balloon flight on 25 September 1993 [*Peterson and Margitan*, 1995]. The latitude (34°N) is close to that of the Wollongong station (34°S). The a priori profile was seasonally adjusted vertically to account for the variation of the local tropopause height. Good fits to the HCl line widths in the measured spectra were achieved throughout the year with this approach.

[67] The stratospheric portion of the a priori profile for $ClONO_2$ was based on an ATMOS version 3 profile [*Irion et al.*, 2002] measured at 32.9°S latitude during March 1992. The $ClONO_2$ mixing ratio profile was spline fitted into a profile that is assumed to be very low (1×10^{-14}) below the seasonally adjusted tropopause.

[68] The low observation altitude and high humidity make the $ClONO_2$ retrievals difficult from Wollongong. A modified wide-narrow, two-step fitting approach [*Reisinger et al.*, 1995] was adopted in the analysis. The retrievals were performed at the reduced resolution of 0.02 cm^{-1} to boost the signal-to-noise ratio following the approach adopted for the Lauder analysis. Zero-level offset corrections were also applied from measurements in saturated spectral regions to correct for the nonlinearity of the HgCdTe detector. Highly temperature sensitive CO_2 lines at 927.0083, 932.9604, and 936.8037 cm^{-1} were fitted simultaneously in the first step to retrieve the CO_2 mixing ratio profile. The revised method takes advantage of higher temperature sensitivity and the improved signal-to-noise of these lines relative to the 780.5035-cm^{-1} CO_2 line adopted for this purpose by *Reisinger et al.* [1995]. Although higher temperature sensitivity is normally a disadvantage, it is not for this particular application as the three CO_2 lines more closely match the temperature sensitivity of the CO_2 line overlapping the $ClONO_2$ 780.2-cm^{-1} Q branch.

A9. Kiruna (67.84°N, 20.41°E, 0.419 km a.s.l.)

[69] Measurements from Kiruna are performed with a Bruker 120HR FTIR spectrometer operated by the Forschungszentrum Karlsruhe and the Institute of Space Physics IRF in collaboration with the University of Nagoya, Japan. The HCl and $ClONO_2$ measurements are performed consecutively, with InSb and HgCdTe detectors, respectively, using the recommended NDSC filter sets. The HgCdTe measurements are corrected for a smooth baseline offset due to nonlinear detector response on the order of a few percent by interpolating between saturated absorption features. Spectra were recorded with resolutions corre-

sponding to maximal OPDs (OPD$_{max}$) of 180 or 257 cm. No numerical apodization is applied. The spectra are resampled to a spectral grid of width equal to $1/(2OPD_{max})$ before the analysis to ensure a diagonal noise covariance and to avoid unnecessary computational effort. Over the whole measurement period, the instrumental lineshape was monitored by regular low-pressure gas cell measurements, which were analyzed with the software LINEFIT [*Hase et al.*, 1999]. Observations are made at least once a week so that, on average, monthly means are based on four or more measurement days.

[70] The analysis of the spectra relies mainly on the HITRAN 2001 spectroscopic database (available at http://www.hitran.com). Spectroscopic parameters derived by *Wagner et al.* [2000] provided better fits to the O_3 signatures in the $ClONO_2$ region than those on the current HITRAN database, and therefore were adopted. For $ClONO_2$ itself, the cross-section data determined by *Birk and Wagner* [2000] were assumed. The cross-section data were interpolated to relevant pressure-temperature grid points using a tool distributed by Birk, and these interpolated values were used directly. The temperature dependence of the partition function was calculated for the line data species using the parameterization of Gamache [*Rothman et al.*, 1998].

[71] The analysis was performed with the retrieval code PROFFIT developed by *Hase* [2000]. This code is similar to SFIT2, but retrieves profiles on a logarithmic volume mixing ratio scale. The radiative transfer code used is KOPRA [*Höpfner et al.*, 1998; *Kuntz et al.*, 1998; *Stiller et al.*, 1998]. NCEP temperature profiles, smoothly merged with the CIRA86 climatology (http://badc.rl.ac.uk/data/cira) above 45 km, were used for the analysis.

[72] The retrieval of HCl used the microwindows 2775.69–2775.84 and 2925.76–2926.04 cm^{-1}. First, the interfering lines of O_3, N_2O, and CH_4 were fitted in appropriate microwindows, then a joint retrieval of O_3 (scaling), CH_4 (scaling), and HCl (profile retrieval) was performed in the above microwindows.

[73] The retrieval approach of $ClONO_2$ first involves retrieving volume mixing ratio profiles of the interfering gases O_3, HNO_3, and H_2O in appropriate microwindows, followed by a joint retrieval of H_2O (scaling), CO_2 (profile retrieval), O_3 (scaling), and $ClONO_2$ (profile retrieval) in the 779.9–780.66 cm^{-1} microwindow. The CO_2 profile is fitted to compensate for deviations from the theoretical line shape. But the HCl and $ClONO_2$ profiles are constrained by forcing them to the assumed climatological mean values at the bottom and top levels of the model atmosphere and by minimizing the first derivative with respect to altitudes in between. Climatological mean profiles from G. C. Toon (private communication, 1998) were adopted.

References

Abrams, M. C., G. C. Toon, and R. A. Schindler, Practical example of the correction of Fourier-transform spectra for detector nonlinearity, *Appl. Opt.*, *33*, 6307–6314, 1994.

Ackerman, M., D. Frimout, A. Girard, M. Gottignies, and C. Muller, Stratospheric HCl from infrared spectra, *Geophys. Res. Lett.*, *3*, 81–83, 1976.

Anderson, J., J. M. Russell III, S. Solomon, and L. E. Deaver, Halogen occultation experiment confirmation of stratospheric chlorine decreases in accordance with the Montreal protocol, *J. Geophys. Res.*, *105*, 4483–4490, 2000.

Ballard, J., W. B. Johnston, M. R. Gunson, and P. T. Wassell, Absolute absorption coefficients of $ClONO_2$ infrared bands at stratospheric temperatures, *J. Geophys. Res.*, *93*, 1659–1665, 1988.

Bell, W., G. Duxbury, and D. D. Stuart, High-resolution spectra of the v_4 band of chlorine nitrate, *J. Mol. Spectrosc.*, *152*, 283–297, 1992.

Birk, M., and G. Wagner, A new spectroscopic database for chlorine nitrate, poster presented at Sixth Biennial Hitran Database Conference, Harvard-Smithsonian Cent. for Astrophys., Cambridge, Mass., 19–21 June 2000.

Brasseur, G., M. H. Hitchman, S. Walters, M. Dymek, E. Falise, and M. Pirre, An interactive chemical dynamical two-dimensional model of the middle atmosphere, *J. Geophys. Res.*, *95*, 5639–5655, 1990.

Brault, J. W., Solar Fourier transform spectroscopy, in *Proceedings of the JOSO Workshop, Future Solar Optical Observations, Needs and Constraints*, edited by G. Godoli, G. Noci, and A. Righin, pp. 33–52, Florence, Italy, 1978.

Brinksma, E. J., et al., Analysis of record-low ozone values during the 1997 winter over Lauder, New Zealand, *Geophys. Res. Lett.*, *25*, 2785–2788, 1998.

Chipperfield, M. P., Multiannual simulations with a three-dimensional chemical transport model, *J. Geophys. Res.*, *104*, 1781–1805, 1999.

Cicerone, R. J., Halogens in the atmosphere, *Rev. Geophys.*, *19*, 123–139, 1981.

Cleveland, W. S., and S. J. Devlin, Locally-weighted regression: An approach to regression analysis by local fitting, *JASA J. Am. Stat. Assoc.*, *83*, 596–610, 1988.

Coffey, M. T., Observations of the impact of volcanic activity on stratospheric chemistry, *J. Geophys. Res.*, *101*, 6767–6780, 1996.

Committee on Extension of the U. S. Standard Atmosphere (COESTA), *U. S. Standard Atmosphere 1976*, 227 pp., Govt. Print. Off., Washington, D. C., 1976.

Connor, B. J., A. Parrish, J.-J. Tsou, and M. P. McCormick, Error analysis for the ground-based microwave ozone measurements during STOIC, *J. Geophys. Res.*, *100*, 9283–9291, 1995.

Connor, B. J., N. B. Jones, S. W. Wood, J. G. Keys, C. P. Rinsland, and F. J. Murcray, Retrieval of HCl and HNO_3 profiles from ground-based FTIR data using SFIT2, in *Proceedings of 18th Quadrennial Ozone Symposium*, edited by R. Bojkov and G. Visconti, pp. 485–488, Parco Sci. e Technol. D'Abruzzo, L'Aquila, Italy, 1996.

Considine, G. D., L. E. Deaver, E. E. Remsberg, and J. M. Russell III, Analysis of near-global trends and variability in halogen occultation experiment HF and HCl data in the middle atmosphere, *J. Geophys. Res.*, *104*, 24,297–24,308, 1999.

Crutzen, P. J., I. S. A. Isaksen, and J. R. McAfee, The impact of the chlorocarbon industry on the ozone layer, *J. Geophys. Res.*, *83*, 345–363, 1978.

Douglass, A. R., M. R. Schoeberl, R. S. Stolarski, J. W. Waters, J. M. Russell III, A. E. Roche, and S. T. Massie, Interhemispheric differences in springtime production of HCl and $ClONO_2$ in the polar vortices, *J. Geophys. Res.*, *100*, 13,967–13,978, 1995.

Engel, A., M. M. Strunk, M. Müller, H.-P. Haase, C. Poss, I. Levin, and U. Schmidt, Temporal development of total chlorine in the high-latitude

stratosphere based on reference distributions of mean age derived from CO_2 and SF_6, *J. Geophys. Res.*, *107*(D12), 4136, doi:10.1029/2001JD000584, 2002.

Farmer, C. B., O. F. Raper, and R. H. Norton, Spectroscopic detection and vertical distribution of HCl in the troposphere and stratosphere, *Geophys. Res. Lett.*, *3*, 13–16, 1976.

Farmer, C. B., G. C. Toon, P. W. Schaper, J.-F. Blavier, and L. L. Lowes, Stratospheric trace gases in the spring 1986 Antarctic atmosphere, *Nature*, *329*, 126–130, 1987.

Gallery, W. O., F. X. Kneizys, and S. A. Clough, Air mass computer program for atmospheric transmittance/radiance calculation: FSCATM, *Environ. Res. Pap.828(AFGL-TR-83-0065)*, 145 pp., Opt. Phys. Div., U.S. Air Force Geophys. Lab., Bedford, Mass., 1983.

Goldman, A., C. Paton Walsh, W. Bell, G. C. Toon, J.-F. Blavier, B. Sen, M. T. Coffey, J. W. Hannigan, and W. G. Mankin, Network for the detection of stratospheric change Fourier transform infrared intercomparison at Table Mountain Facility, November 1996, *J. Geophys. Res.*, *104*, 30,481–30,503, 1999.

Griffith, D. W. T., N. B. Jones, and W. A. Mathews, Interhemispheric ratio and annual cycle of carbonyl sulfide (OCS) total column from ground-based solar FTIR spectra, *J. Geophys. Res.*, *103*, 8447–8454, 1998.

Gunson, M. R., M. C. Abrams, L. L. Lowes, E. Mahieu, R. Zander, C. P. Rinsland, M. K. W. Ko, N. D. Sze, and D. K. Weisenstein, Increase in levels of stratospheric chlorine and fluorine loading between 1985 and 1992, *Geophys. Res. Lett.*, *21*, 2223–2226, 1994.

Hase, F., Retrieval of trace gas profiles from high resolution, ground-based FTIR measurements, Ph.D. thesis, Wissenschaftliche Berichte FZKA6512, Forschungszentrum Karlsruhe, 2000.

Hase, F., T. Blumenstock, and C. Paton-Walsh, Analysis of the instrumental line shape of high-resolution Fourier transform IR spectrometers with gas cell measurements and new retrieval software, *Appl. Opt.*, *38*, 3417–3422, 1999.

Höpfner, M., G. P. Stiller, T. Kuntz, T. v. Clarmann, G. Echle, B. Funke, N. Glattohr, F. Hase, H. Kemnitzer, and S. Zorn, Karlsruhe optimized and precise radiative transfer algorithm, II, Interface to retrieval applications, in *Optical Remote Sensing of the Atmosphere and Clouds*, edited by J. Wang et al., *Proc. SPIE 3501*, 186–195, 1998.

Irion, F. W., et al., The Atmospheric Trace Molecule Spectroscopy Experiment (ATMOS) version 3 data retrievals, *Appl. Opt.*, *41*, 6968–6979, 2002.

Jackman, C. H., E. L. Fleming, S. Chandra, D. B. Considine, and J. E. Rosenfield, Past, present, and future modeled ozone trends with comparisons to observed trends, *J. Geophys. Res.*, *101*, 28,753–28,767, 1996.

Kinnersley, J. S., The climatology of the stratospheric "thin air" model, *Q. J. R. Meteorol. Soc.*, *122*, 219–252, 1996.

Koike, M., N. B. Jones, W. A. Matthews, P. V. Johnston, R. L. McKenzie, D. Kinnison, and J. Rodriguez, Impact of Pinatubo aerosols on the partitioning between NO_2 and HNO_3, *Geophys. Res. Lett.*, *21*, 597–600, 1994.

Kuntz, M., M. Höpfner, G. P. Stiller, T. v. Clarmann, H. Echle, B. Funke, N. Glattohr, F. Hase, H. Kemnitzer, and S. Zorn, Karlsruhe optimized and precise radiative transfer algorithm, III, ADDLIN and TRANSF algorithms for modeling spectral transmittance and radiance, in *Optical Remote Sensing of the Atmosphere and Clouds*, edited by J. Wang et al., *Proc. SPIE3501*, 247–256, 1998.

Kurylo, M. J., Network for the detection of stratospheric change (NDSC), *Proc. Soc. Photo-Opt. Instrum. Eng.*, *1491*, 168–174, 1991.

Kurylo, M. J., and R. J. Zander, The NDSC—Its status after 10 years of operation, paper presented at 19th Quadrennial Ozone Symposium, Hokkaido Univ., Sapporo, Japan, 3–8 July 2000.

Mahieu, E., R. Zander, L. Delbouille, P. Demoulin, G. Roland, and C. Servais, Observed trends in total vertical column abundances of atmospheric gases from IR solar spectra recorded at the Jungfraujoch, *J. Atmos. Chem.*, *28*, 227–243, 1997.

Mahieu, E., R. Zander, P. Demoulin, F. De Mazière, F. Mélen, C. Servais, G. Roland, L. Delbouille, J. Poels, and R. Blomme, Fifteen years-trend characteristics of key stratospheric constituents monitored by FTIR above the Jungfraujoch, in *Proceedings of the 5th European Symposium on Stratospheric Ozone, Air Pollut. Res. Rep. 73—EUR 19340*, edited by N. R. P. Harris, M. Guirlet, and G. T. Amanatidis, pp. 99–102, Eur. Ozone Res. Coord. Unit, Cambridge, UK, 2000.

Mankin, W. G., and M. T. Coffey, Latitudinal distributions and temporal changes of stratospheric HCl and HF, *J. Geophys. Res.*, *88*, 10,776–10,784, 1983.

Mankin, W. G., and M. T. Coffey, Increased stratospheric hydrogen chloride in the El Chichón cloud, *Science*, *226*, 170–172, 1984.

Mankin, W. G., M. T. Coffey, and A. Goldman, Airborne observations of SO_2, HCl, and O_3 in the stratospheric plume of the Pinatubo volcano in July 1991, *Geophys. Res. Lett.*, *19*, 179–182, 1992.

Matthews, W. A., P. V. Johnson, D. G. Murcray, F. J. Murcray, and R. D. Blatherwick, Column abundances of hydrogen chloride above Lauder, New Zealand, in *Ozone in the Atmosphere*, edited by R. D. Bojkov and P. Fabian, pp. 359–361, A. Deepak, Hampton, Va., 1989.

Meier, A., A. Goldman, P. S. Manning, T. M. Stephen, C. P. Rinsland, N. B. Jones, and S. W. Wood, Improvements to air mass calculations from ground-based infrared measurements, *J. Quant. Spectrosc. Radiat. Transfer*, in press, 2003.

Michelsen, H. A., C. M. Spivakovsky, and S. C. Wofsy, Aerosol-mediated partitioning of stratospheric Cl_y and NO_y at temperatures above 200 K, *Geophys. Res. Lett.*, *26*, 299–302, 1999.

Molina, M. J., and F. S. Rowland, Stratospheric sink for chlorofluoromethanes: Chlorine atom-catalysed destruction of ozone, *Nature*, *249*, 810–812, 1974.

Montzka, S. A., J. H. Butler, R. C. Myers, T. M. Thompson, T. H. Swanson, A. D. Clarke, L. T. Lock, and J. W. Elkins, Decline in the tropospheric abundance of halogen from halocarbons: Implications for stratospheric ozone depletion, *Science*, *272*, 1318–1322, 1996.

Montzka, S. A., J. H. Butler, J. W. Elkins, T. M. Thompson, A. D. Clarke, and L. T. Lock, Present and future trends in the atmospheric burden of ozone-depleting halogens, *Nature*, *398*, 690–694, 1999.

Murcray, F. J., A. Matthews, A. Goldman, P. Johnston, and C. P. Rinsland, NH_3 column abundances over Lauder, New Zealand, *J. Geophys. Res.*, *94*, 2235–2238, 1989.

Norton, R. J., and C. P. Rinsland, ATMOS data processing and science analysis methods, *Appl. Opt.*, *30*, 389–400, 1991.

Notholt, J., The moon as light source for FTIR measurements of stratospheric trace gases during the polar night: Application for HNO_3 in the Arctic, *J. Geophys. Res.*, *99*, 3607–3614, 1994.

Notholt, J., and O. Schrems, Ground-based FTIR spectroscopic measurements of stratospheric trace gases in the Arctic with the Sun and moon as light sources, *J. Mol. Struct.*, *347*, 407–416, 1995.

Notholt, J., A. Meier, and S. Peil, Total column densities of tropospheric and stratospheric trace gases in the undisturbed arctic summer atmosphere, *J. Atmos. Chem.*, *20*, 311–332, 1995.

Notholt, J., G. C. Toon, F. Stordal, S. Solberg, N. Schmidbauer, E. Becker, A. Meier, and B. Sen, Seasonal variations of atmospheric trace gases in the high arctic at 79°N, *J. Geophys. Res.*, *102*, 12,855–12,861, 1997a.

Notholt, J., G. C. Toon, R. Lehmann, B. Sen, and J.-F. Blavier, Comparison of Arctic and Antarctic trace gas column abundances from ground-based Fourier transform infrared spectrometry, *J. Geophys. Res.*, *102*, 12,863–12,869, 1997b.

Parrish, A., B. J. Connor, J. J. Tsou, I. S. McDermid, and W. G. Chu, Ground-based microwave monitoring of stratospheric ozone, *J. Geophys. Res.*, *97*, 2541–2546, 1992.

Penkett, S. A., R. G. Derwent, P. Fabian, R. Borchers, and U. Schmidt, Methyl chloride in the stratosphere, *Nature*, *283*, 58–60, 1980.

Peterson, D. B., and J. M. Margitan (Eds.), *Upper Atmosphere Research Satellite Correlative Measurements Program (UARS-CMP) Balloon Data Atlas*, NASA, Washington, D. C., 1995.

Pougatchev, N. S., B. J. Connor, and C. P. Rinsland, Infrared measurements of the ozone vertical distribution above Kitt Peak, *J. Geophys. Res.*, *100*, 16,689–16,697, 1995.

Prinn, R. G., et al., A history of chemically and radiatively important gases in air deduced from ALE/GAGE/AGAGE, *J. Geophys. Res.*, *105*, 17,751–17,792, 2000.

Randel, W. J., F. Wu, J. M. Russell, and J. W. Waters, Space-time patterns of trends in stratospheric constituents derived from UARS measurements, *J. Geophys. Res.*, *104*, 3711–3727, 1999.

Raper, O. F., C. B. Farmer, R. Zander, and J. H. Park, Infrared spectroscopic measurements of halogenated sink and reservoir gases in the stratosphere with the ATMOS instrument, *J. Geophys. Res.*, *92*, 9851–9858, 1987.

Reisinger, A. R., N. B. Jones, W. A. Matthews, and C. P. Rinsland, Southern hemisphere midlatitude ground based measurements of $ClONO_2$: Method of analysis, seasonal cycle and long-term trend, *J. Geophys. Res.*, *100*, 23,183–23,193, 1995.

Rinsland, C. P., M. A. H. Smith, P. L. Rinsland, A. Goldman, J. W. Brault, and G. M. Stokes, Ground-based infrared spectroscopic measurements of atmospheric hydrogen cyanide, *J. Geophys. Res.*, *87*, 11,119–11,125, 1982.

Rinsland, C. P., A. Goldman, F. J. Murcray, F. H. Murcray, R. D. Blatherwick, and D. G. Murcray, Infrared measurements of atmospheric gases above Mauna Loa, Hawaii, in February 1987, *J. Geophys. Res.*, *91*, 12,607–12,626, 1988.

Rinsland, C. P., J. S. Levine, A. Goldman, N. D. Sze, M. K. W. Ko, and D. W. Johnson, Infrared measurements of HF and HCl total column abundances above Kitt Peak, 1977–1990: Seasonal cycles, long-term increases, and comparisons with model calculations, *J. Geophys. Res.*, *96*, 15,523–15,540, 1991.

Rinsland, C. P., M. R. Gunson, M. C. Abrams, R. Zander, E. Mahieu, A. Goldman, M. K. W. Ko, J. M. Rodriguez, and N. D. Sze, Profiles of stratospheric chlorine nitrate (ClONO$_2$) from atmospheric trace molecule spectroscopy/ATLAS 1 infrared solar occultation spectra, *J. Geophys. Res.*, *99*, 18,895–18,900, 1994.

Rinsland, C. P., R. Zander, P. Demoulin, and E. Mahieu, ClONO$_2$ total vertical column abundances above the Jungfraujoch station: 1986–1994: Long-term trend and winter-spring enhancements, *J. Geophys. Res.*, *101*, 3891–3899, 1996.

Rinsland, C. P., et al., Northern and Southern hemisphere ground-based infrared spectroscopic measurements of tropospheric carbon monoxide and ethane, *J. Geophys. Res.*, *103*, 28,197–28,217, 1998.

Rinsland, C. P., et al., Infrared solar spectroscopic measurements of free tropospheric CO, C$_2$H$_6$, and HCN above Mauna Loa, Hawaii: Seasonal variations and evidence for enhanced emissions from the southeast Asian tropical fires of 1997–1998, *J. Geophys. Res.*, *104*, 18,667–18,680, 1999.

Rinsland, C. P., E. Mahieu, R. Zander, P. Demoulin, J. Forrer, and B. Buchmann, Free tropospheric CO, C$_2$H$_6$, and HCN above central Europe: Recent measurements from the Jungfraujoch station including the detection of elevated columns during 1998, *J. Geophys. Res.*, *105*, 24,235–24,249, 2000a.

Rinsland, C. P., et al., Correlation relationships of stratospheric molecular constituents from high spectral resolution, ground-based infrared solar absorption spectra, *J. Geophys. Res.*, *105*, 14,637–14,652, 2000b.

Rinsland, C. P., A. Meier, and D. W. T. Griffith, Ground-based measurements of tropospheric CO, C$_2$H$_6$, and HCN from Australia at 34°S latitude during 1997–1998, *J. Geophys. Res.*, *106*, 20,913–20,924, 2001.

Rodgers, C. D., Characterization and error analysis of profiles retrieved from remote sounding measurements, *J. Geophys. Res.*, *95*, 5587–5595, 1990.

Rothman, L. S., et al., The HITRAN molecular database: Editions of 1991 and 1992, *J. Quant. Spectrosc. Radiat. Transfer*, *48*, 469–507, 1992.

Rothman, L. S., et al., The HITRAN molecular spectroscopic database and HAWKS (HITRAN atmospheric workstation), *J. Quant. Spectrosc. Radiat. Transfer*, *60*, 665–710, 1998.

Russell, J. M., III, L. L. Gordley, J. H. Park, S. R. Drayson, D. H. Hesketh, R. J. Cicerone, A. F. Tuck, J. E. Frederick, J. E. Harries, and P. J. Crutzen, The halogen occultation experiment, *J. Geophys. Res.*, *98*, 10,777–10,797, 1993.

Russell, J. M., III, et al., Validation of hydrogen chloride measurements made by the halogen occultation experiment from the UARS platform, *J. eophys. Res.*, *101*, 10,151–10,162, 1996.

Ryan, J. A., and N. R. Mukherjee, Sources of stratospheric gaseous chlorine, *Rev. Geophys.*, *13*, 650–658, 1975.

Solomon, S., R. W. Portmann, R. R. Garcia, W. Randel, F. Wu, R. Nagatani, J. Gleason, L. Thomason, L. R. Poole, and M. P. McCormick, Ozone depletion at mid-latitudes: Coupling of volcanic aerosols and temperature variability to anthropogenic chlorine, *Geophys. Res. Lett.*, *25*, 1871–1874, 1998.

Stiller, G. P., et al., Karlsruhe optimized and precise radiative transfer algorithm, I, Requirements, justification and model error estimation, in *Optical Remote Sensing of the Atmosphere and Clouds*, edited by J. Wang et al., *Proc. SPIE 3501*, 257–268, 1998.

Sussmann, R., Ground-based Fourier transform spectrometry at the NDSC site Zugspitze: Geophysical products for satellite validation, *Proc. Eur. Symp. Atmos. Meas. Space, ESTEC, Noordwijk, The Netherlands, Jan. 18–22 1999*, WPP-161, *2*, 661–664, 1999.

Sussmann, R., and K. Schäfer, Infrared spectroscopy of tropospheric trace gases: Combined analysis of horizontal and vertical column abundances, *Appl. Opt.*, *36*, 735–774, 1997.

Sussmann, R., and W. Wimmer, A subtropical intrusion in February 1998 analyzed by ground-based FTIR spectrometry at the NDSC site Zugspitze at 47.4°N, *Proc. 5th Eur. Workshop on Stratos. Ozone, Air Pollut. Res. Rep. 73*, edited by N. R. P. Harris, M. Guirlet, and G. T. Amanatidis, pp. 594–597, Res. Environ. and Sustain. Dev. Prog., 2000.

Toon, G. C., The JPL MkIV interferometer, *Opt. Photonic News*, *2*, 19–21, 1991.

Toon, G. C., J.-F. Blavier, B. Sen, R. J. Salawitch, G. B. Osterman, J. Notholt, M. Rex, C. T. McElroy, and J. M. Russell III, Ground-based observations of Arctic ozone loss during spring and summer 1997, *J. Geophys. Res.*, *104*, 26,497–26,510, 1999.

Toth, R. A., Water vapor measurements between 590 and 2582 cm^{-1}, *J. Mol. Spectrosc.*, *190*, 379–396, 1998.

Wagner, G., M. Birk, F. Schreier, and J.-F. Flaud, A new spectroscopic database for the ozone fundamentals, paper presented at 6th biennial HITRAN database conference, Harvard-Smithsonian Cent. for Astrophys., Cambridge, Mass., 2000.

Wallace, L., and W. Livingston, Spectroscopic observations of atmospheric trace gases over Kitt Peak, 3, Long-term trends of hydrogen chloride and hydrogen fluoride from 1978 to 1990, *J. Geophys. Res.*, *96*, 15,513–15,521, 1991.

Wallace, L., W. Livingston, and D. N. B. Hall, A twenty-five year record of stratospheric hydrogen chloride, *Geophys. Res. Lett.*, *24*, 2363–2366, 1997.

Waugh, D. W., D. B. Considine, and E. L. Fleming, Is upper stratospheric chlorine decreasing as expected?, *Geophys. Res. Lett.*, *28*, 1187–1190, 2001.

Webster, C. R., H. A. Michelsen, M. R. Gunson, J. J. Margitan, J. M. Russell III, G. C. Toon, and W. A. Traub, Response of lower stratospheric HCl/Cl$_y$ to volcanic aerosol: Observations from aircraft, balloon, space shuttle, and satellite instrumentation, *J. Geophys. Res.*, *105*, 11,711–11,719, 2000.

Wood, S. W., N. B. Jones, C. P. Rinsland, A. Goldman, B. J. Connor, T. M. Stephen, B. N. Lawrence, and F. J. Murcray, Retrieval of vertical trace gas profiles from ground-based infrared absorption spectra inside and outside the Antarctic vortex using SFIT2, paper presented at Spring Meeting, AGU, Boston, Mass., 29 May–2 June 2001.

World Meteorological Organization (WMO), Atmospheric Ozone 1985: Assessment of our understanding of the processes controlling its present distribution and change, in *World Meteorological Organization, Global Ozone Research and Monitoring Project—Rep. 16*, Geneva, 1986.

World Meteorological Organization (WMO), Scientific Assessment of ozone depletion: 1998, in *WMO Rep. 38*, U.N. Environ. Program., Geneva, 1999.

World Meteorological Organization (WMO), Scientific Assessment of ozone depletion: 2002, in *WMO Rep. xx*, U.N. Environmental Programme, Geneva, 2003.

Zander, R., and Ph. Demoulin, Spectroscopic evidence for the presence of the ν_4-Q branch of chlorine nitrate in ground-based infrared solar spectra, *J. Atmos. Chem.*, *6*, 191–200, 1988.

Zander, R., C. P. Rinsland, C. B. Farmer, L. R. Brown, and R. H. Norton, Observation of several chlorine nitrate (ClONO$_2$) bands in stratospheric infrared spectra, *Geophys. Res. Lett.*, *13*, 757–760, 1986.

Zander, R., G. Roland, L. Delbouille, A. Saval, C. B. Farmer, and R. H. Norton, Column abundance and the long-term trend of hydrogen chloride (HCl) above the Jungfraujoch station, *J. Atmos. Chem.*, *5*, 395–404, 1987.

Zander, R., M. R. Gunson, C. B. Farmer, C. P. Rinsland, F. W. Irion, and E. Mahieu, The 1985 chlorine and fluorine inventories in the stratosphere based on ATMOS observations at 30°N latitude, *J. Atmos. Chem.*, *15*, 171–186, 1992.

Zander, R., E. Mahieu, and Ph. Demoulin, Monitoring of stratospheric changes at the Jungfraujoch station by high resolution infrared solar observations in support of the network for the detection of stratospheric change, in *The Role of the Stratosphere in Global Change*, NATO ASI Ser., vol. I 8, edited by M. L. Chanin, Springer-Verlag, New York, 1993a.

Zander, R., P. Demoulin, E. Mahieu, G. P. Adrian, C. P. Rinsland, and A. Goldman, ESMOS II/NDSC IR spectral fitting algorithms intercomparison exercise, in *Proceedings of the Atmospheric Spectroscopic Applications Workshop*, edited by A. Barbe and L. Rothman, pp. 7–12, Univ. of Reims, Champaigne-Ardenne, France, 1993b.

Zander, R., et al., The 1994 northern midlatitude budget of stratospheric chlorine derived from ATMOS/ATLAS-3 observations, *Geophys. Res. Lett.*, *23*, 2357–2360, 1996.

Zander, R., P. Demoulin, E. Mahieu, L. Delbouille, G. Roland, F. Mélen, C. Servais, M. De Mazière, and M. Van Roozendael, An overview of NDSC-related activities at the Jungfraujoch through high-resolution infrared solar observations, in *Atmospheric Ozone: Proceedings of the 28th Quadrennial Ozone symposium*, edited by R. D. Bojkov and G. Visconti, pp. 1005–1008, Parco Sci. e Technol. D'Abruzzo, L'Aquila, Italy, 1998.

Zander, R., P. M. Midgley, and M. J. Kurylo, The NDSC in support of satellite data validation and calibration, in *Proc. of ESAMS '99—Eur. Symp. on Atmos. Meas. from Space—ESTEC, Noordwijk, 19–22 Jan. 1999*, WPP-161, *2*, 649–654, 1999.

———————

J. Anderson and J. M. Russell III, Department of Physics, Center for Atmospheric Sciences, Hampton University, 23 Tyler St., Hampton, VA 23668, USA. (john.anderson@hamptonu.edu; james.russell@hamptonu.edu)

J.-F. Blavier, B. Sen, and G. C. Toon, Jet Propulsion Laboratory, California Institute of Technology, Pasadena, CA 91109, USA. (jeanfrancois.l.blavier@jpl.nasa.gov; bhaswar.sen@jpl.nasa.gov; geoffrey.c.toon@jpl.nasa.gov)

T. Blumenstock, F. Hase, and S. Mikuteit, Institute of Meteorology and Climate Research, Atmospheric Environmental Research IMK-ASF, Forschungszentrum Karlsruhe, GmbH, Postfoch 76021, Karlsruhe, Germany. (thomas.blumenstock@imk.fzk.de; frank.hase@imk.fzk.de; sabine.mikuteit@imk.fzk.de)

L. S. Chiou, Science Application International Corporation, One Enterprise Parkway, Hampton, VA 23666-1498, USA. (l.s.chiou@larc.nasa.gov)

M. P. Chipperfield, School of the Environment, University of Leeds, Leeds, LS2 9JT, UK. (martyn@env.leeds.ac.uk)

P. Demoulin, E. Mahieu, and R. Zander, Institute of Astrophysics and Geophysics, University of Liège, 17 Allée du 6 Août, 4000, Liège, Belgium. (demoulin@astro.ulg.ac.be; emmanuel.mahieu@ulg.ac.be; r.zander@ulg.ac.be)

A. Goldman, F. J. Murcray, and T. M. Stephen, Department of Physics, University of Denver, Denver, CO 80208, USA. (goldman@acd.ucar.edu; fmurcray@du.edu; tstephen@du.edu)

D. W. T. Griffith, N. B. Jones, and A. Meier, Department of Chemistry, University of Wollongong, Northfields Avenue, Wollongong, New South Wales, 2522, Australia. (njones@uow.edu.au; griffith@uow.edu.au; arndt@uow.edu.au)

J. Notholt, Institute of Environmental Physics, University of Bremen-FB1, Postfach 1, 330440 D-28334, Bremen, Germany. (jnotholt@iup.physik.uni-bremen.de)

C. P. Rinsland, NASA Langley Research Center, Mail Stop 402, 21 Langley Boulevard, Hampton, VA 23681-2199, USA. (c.p.rinsland@larc.nasa.gov)

A. Schulz, Alfred Wegener Institute for Polar and Marine Research, Telegraphenberg A43, 14473, Potsdam, Germany. (aschulz@awi-potsdam.de)

R. Sussmann, Institute of Meteorology and Climate Research IMK-IFU, Forschungszentrum Karlsruhe, GmbH, Kreuzeckbahnstrasse 19, D-82467, Garmisch-Partenkirchen, Germany. (ralf.sussmann@imk.fzk.de)

S. W. Wood, NIWA Climate, Private Bag 50061, Omakau, Central Otago, New Zealand. (s.wood@niwa.cri.nz)